DIPLOMA THESIS

Parameter Estimation Based on Back Analysis of Measured Displacement Data in the Inntal Tunnel Project

JUAN MANUEL DAVILA MENDEZ

Institute for Rock Mechanics and Tunneling
Graz University of Technology

Advisors:

O.Univ.-Prof. Dipl.-Ing. Dr.mont. Wulf Schubert
Institute for Rock Mechanics and Tunneling
Graz University of Technology

Dipl.-Ing. Corina Leber
Institute for Rock Mechanics and Tunneling
Graz University of Technology

Graz, June 2010

Declaration

I declare in lieu of oath that I did this thesis in hand by myself using only literature cited at the end of this work.

Graz, June 2010 Juan Manuel Davila Mendez

ACKNOWLEDGMENTS

I would like to express my sincere appreciation and gratitude to O.Univ.-Prof. Dipl.-Ing. Dr.mont. Wolf Schubert and to my supervisor Dipl.-Ing. Corina Leber for their kind supervision, invaluable suggestions and help towards the completion of my Thesis.

My special gratitude and appreciation is extended to Ass.Prof. Dipl.-Ing. Dr.techn. Manfred Blümel, Dipl.-Ing.Thomas Pilgerstorfer and Dipl.-Ing. Nedim Radoncic for their valuable suggestions, help and kindnesses during the completion of this thesis.

Finally, I wish to express my sincere gratitude to my dear family especially my lovely parents for their continuing love and support. I would not have achieved this goal without their patience, understanding and encouragement. To whom, I dedicate this thesis.

ABSTRACT

The Convergence-Confinement Method has been used with success in tunnel design and it is nowadays considered a useful tool for the assessment of system behaviour. The method allows an approximate transformation of a four dimensional (spatial and temporal) problem, into a graphical, two-dimensional description of the system behaviour by using a Ground reaction Curve (GRC), Support Characteristic Curve (SCC) and the Longitudinal Deformation Profile (LDP). Its applicability is limited to conditions of high overburden and weak rock masses.

This study represents a practical application of the Convergence-Confinement Method for back analysis of rock mass properties. It is assumed that the rock mass satisfies the Mohr Coulomb failure criterion. The MATLAB code developed for the back analysis accounts for different support systems and their combinations, including shotcrete, non grouted bolts–cables, grouted bolts, open displacement gaps, lining stress controllers and steel profiles. The measured displacements are used as input values, and the rock mass parameters are varied until the final displacements and the longitudinal displacement profile are best fitting the measured data. This procedure was implemented in Matlab allowing several calculations for different values of Young's modulus (E), cohesion (c), and friction angle (φ) to take place relatively fast. Combined values, which are in agreement with the measured displacements, are saved and later put to scrutiny.

The Inntal tunnel was used to apply the model. The project was selected based on the amount and quality of convergence data.

At the end of this study a discussion and conclusions are presented, mainly focusing on the usage of the convergence-confined method, comparisons of the proposed model with the formulation from Feder & Arwanitakis [1] and Finite Element (FE) simulations, comparisons between support systems, influence of

Young’s moduli on the back analyzed parameters and the results for the specific study case.

Kurzfassung

Das Kennlinienverfahren wird seit vielen Jahren erfolgreich in der Planung von Tunnelbauten eingesetzt und stellt ein nützliches Element zur Bestimmung des Systemverhaltens dar. Es ermöglicht ein vierdimensionales Problem (in Raum und Zeit) in eine graphische zweidimensionale Darstellung unter Verwendung von Gebirgskennlinie (Ground Reaction Curve GRC), Ausbaukennlinie (Support Characteristic Curve SCC) und der Tunnellängsentwicklung der radialen Verformungen (Longitudinal Deformation Profile LDP) zu transformieren. Das Verfahren ist jedoch nur begrenzt anwendbar in Fällen mit hoher Überlagerung und schwachem Gebirge.

In dieser Arbeit wird eine praktische Anwendung zur Rückrechnung der Gebirgsparameter mittels Kennlinienverfahren vorgestellt, wobei angenommen wird, dass das Gebirge dem Mohr Coulomb'schen Fehlerkriterium folgt. Der für die Rückrechnung entwickelte Matlab Code ist für verschiedene Stützmittel wie Spritzbeton, Freispielanker, Verbundanker, offene Verformungsschlitze, Stauchelemente, Stahlprofile und deren Kombinationen anwendbar. Die Verschiebungsmessdaten werden als Eingangsparameter verwendet, unter Variation der Gebirgsparameter wird versucht jene Kombination zu finden, bei der die errechneten Verschiebungen und das LDP (Longitudinal Deformation Profile) jenen gemessenen Verschiebungsdaten entsprechen. Diese Prozedur wurde in eine Matlab Entwicklung implementiert, die es erlaubt sämtliche Rechnungen für verschiedene Werte von Elastizitätsmodul (E), Kohäsion (c) und Reibungswinkel (φ) in kurzer Zeit durchzuspielen. Die Parameter aus Kombinationen, die jene, den gemessenen Daten entsprechenden, Verschiebungen erzeugen, werden für weitere Untersuchungen gespeichert.

Das erarbeitete Modell wurde am Inntal Tunnel Projekt angewandt, welches aufgrund der Qualität und Quantität der Messdaten ausgewählt wurde.

Diese Arbeit konzentriert sich auf die Anwendung des Kennlinienverfahrens, den Vergleich jenes Modells mit Formulierung nach Feder et al. [17] mit Finite Elemente Simulationen, den Vergleich unterschiedlicher Stützmittel, den Einfluss von Elastizitätsmodul auf die rückgerechneten Parameter und die Ergebnisse der speziellen Studie.

Abbreviations

φ_r	Residual friction angle
τ	Shear strength / stress
E	Young's Modulus
c	Cohesion
φ	Friction angle
ψ	Creep coefficient
R_{adm}	Admissible error
K_o	lateral earth pressure coefficient
H	Overburden

GRC	Ground Reaction Curve
SCC	Support Characteristic Curve
DBBA	Displacement Based Back Analysis
UDEC	Universal Distinct Element Code
FDM	Finite Difference Method
FEM	Finite Element Method
BEM	Boundary Element Method
SVM	Support Vector Machines
SMO	Sequential Minimal Optimization
NATM	New Austrian Tunneling Method
LSC	Lining Stress Controller
BAA	Back Analysis Algorithm
DEM	Displacement Evaluation Model
DBAP	Direct Back Analysis Program
BANSJI	Back Analysis of Non-Linear Strains for Jointed rock mass in Incremental form

Table of contents

Figures – Photographs and Tables

1. Introduction

1.1. Problem description and aim of this work

Engineering means constantly searching and developing new methods and models in order to approach problems in a better and more accurate way. For the specific case of tunneling and underground constructions all project phases – especially design and construction- are filled with a wide range of uncertainties, which add more complexity to the problem. Engineers, in pursuit of both technical and economical solutions are driven into simplifications that often mislead to non-optimal solutions. Strong effort has been made to minimize this simplifications and uncertainties, better approach, sampling methods, monitoring, laboratory testing, numerical methods, higher order models, etc. are used for this purpose, but does one obtain accurate ground condition?

Displacement Based Back Analysis (DBBA) in tunneling is an indirect technique that attempts to find ground conditions (properties), based on monitored data. Clear advantages of this technique are to be seen. On the one hand, engineers are able to evaluate and predict equivalent mechanical constants of the ground that reflect the effects of cracks, joints and the non-linearity of the tunnel movements [2] and on the other hand, parameters can be continuously adjusted throughout a project. Based on the above written and due to its simplicity and maturity the DBBA has become a strong and widely used tool in tunneling and underground construction.

The main purpose of this thesis is to compare the Young's modulus, cohesion and internal friction angle considered for design – often based on laboratory and In situ testing - with those back calculated through DBBA; this is done by using the convergence-confinement method to implement the DBBA technique in the Inntal Tunnel project located in Austria, where a good monitoring program took place.

Xia-Ting et al. [3] and Fakhimi et al. [4] stated the importance of quantity and quality of monitoring data for the DBBA to work, it is shown that accuracy increases in a high degree with the quantity of monitored data, in order to avoid extrapolation and engineering judgments.

1.2. Literature review

Tunneling design is based on in-situ stresses as well as behavior and mechanical properties of surrounding rock masses, complications arise due to the fact that only small samples (cores) are tested to represent rock mass parameters and in situ stresses are calculated by using geological investigation and bore hole testing, leaving plenty of uncertainties behind. DBBA represents an interesting tool to optimize this rock mass properties - obtained by laboratory or in-situ testing - on projects where displacement data is available, as written by Oreste [5], DBBA can only be performed during or/and after the construction of the tunnel itself or of a pilot tunnel, since only in these stages it is possible to obtain a complete evaluation of the behavior of the rock mass based on displacements. Many researches have been made and papers have been written on DBBA for tunneling. [6] A wide range of Back Analysis procedures is available for tunnel engineering and one can say that all procedures follow the flow chart shown in Fig. 1. Differences lie in the selection of displacement evaluation model, the method used for the error calculation and the Back Analysis Algorithm (BAA) selected in order to minimize the error.

Regarding Displacement Evaluation Model, the error calculation and the BAA a number of models are proposed, for instance Shang et al. in [7] and [8] use the computational program BMP90 based on the Boundary Element Method (BEM) for the displacement calculation, the least square method for the error calculation and an intelligent back analysis algorithm which is based on the experiences of a tunnel expert or regulation grouping. Even though this method has shown good results one can observe disadvantages when comparing it to algorithms used by other

authors, as an expert or a board has to be present when the new input parameters are to be selected, giving this method less performance compared to other proposed methods.

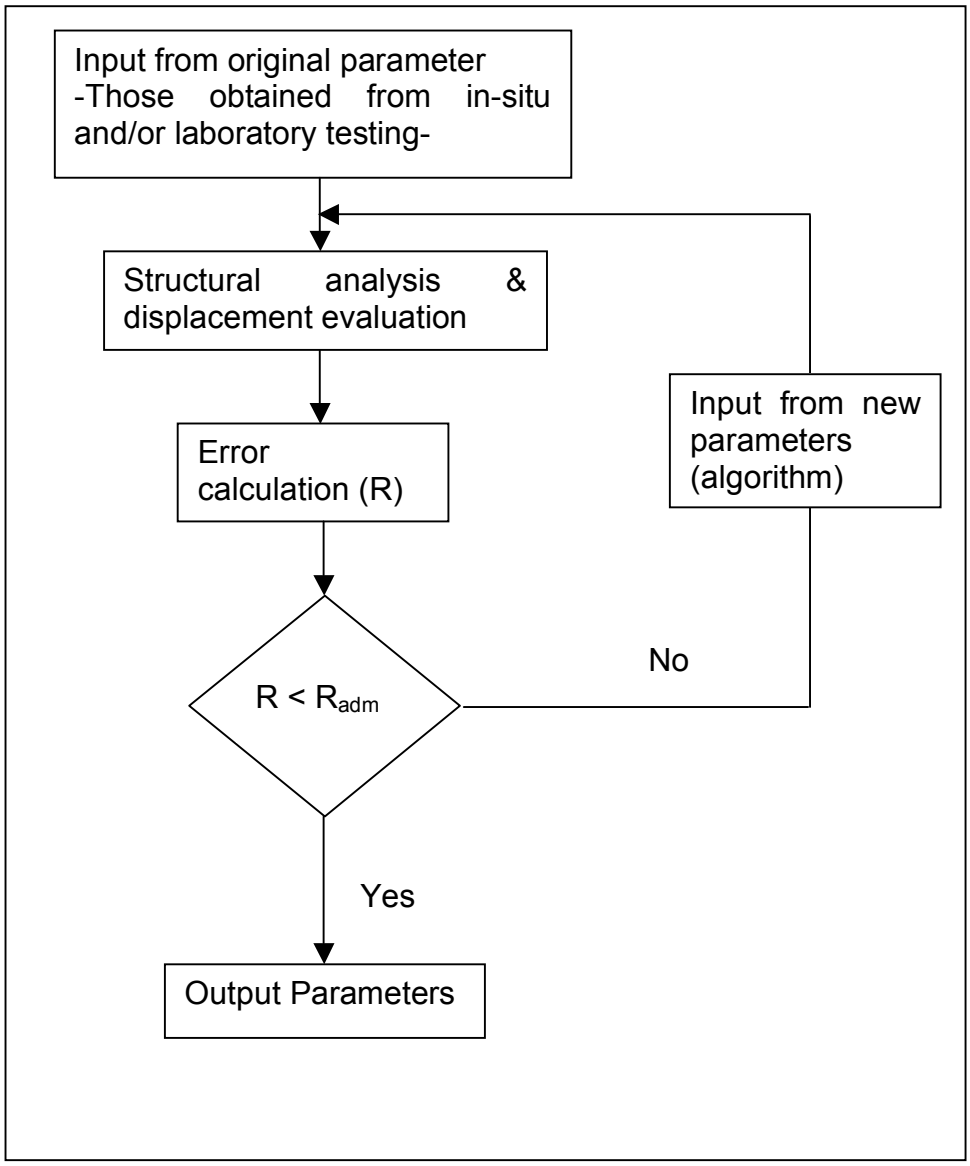

Fig. 1: Back Analysis Flow Chart

Vardakos et al. [9] use the convergence-confinement method and transform it to be implemented in the Discrete Element Method (DEM) based Program UDEC (Universal Distinct Element Code), the computational program corrects itself by

means of the so called Loss Factor “λi”. This factor is linked to the displacements and rock mass properties therefore when equilibrium is reached in between predicted displacements and measured displacements the process stops and the output parameters are read out. Due to the non-continuous model form UDEC and the convergence-confinement method a good representation of faults, fractures, joints, bending planes as well as support and construction stages can be realized, however this calculation is time-consuming.

Hisatake & Hieda in [2] used a 3D Finite Element Method (3DFEM), the error calculation and new parameter selection is performed by using the secant method. The method has only been used for elastic ground models, nevertheless it enables prediction of mechanical characteristics of the material ahead of the tunnel face.

The computational Program FLAC, based on the Finite Difference Method (FDM) is used by Fakhimi et al. [4]. The error calculation was performed by the least square method while the correction for the input parameters was done by an expert. Despite some data collection problems, that the authors had to face in this specific project (Resalat Tunnel), good approximations were obtained.

Amusin et al. [10] used the computational program NEDRA based on theoretical empirical method. The proposed back analysis method has three empirical correction factors “X_i“ based on the measured displacements, each factor has to be multiplied with a specific parameter: X_1 with “Q” (in-situ stresses), X_2 with “R” (rock mass strength) and X_3 with “ψ” (creep coefficient). The iteration of this procedure leads to the output parameters.

A combination of the observational method and computational algorithms is used by Shunsuke et al. [6]. The so called Direct Back Analysis Program (DBAP) allows the engineer to roughly approximate ground parameters by using a linear elastic material to associate measured displacements and normalized in-situ stress components. By using this program one can calibrate the model; the second

algorithm is the so called Back Analysis of Non-Linear Strains for Jointed rock mass in Incremental form (BANSJI). Using this algorithm the designer can achieve a more realistic approach to the rock mass behavior. A significant feature of this procedure is the implementation of the observational method, which enables not only to calibrate the parameters but also the model itself.

Oreste in [5] and [11] utilizes the convergence-confinement method and the secant method for displacement prediction and the least square method is used to calculate the error. The approach proposed by Oreste for the DBBA uses vectorial formulation, the gradient method and successive approximations, through these techniques the new input parameters are recalculated. There are pros and cons regarding the convergence-confinement method. On the one hand certain parameters can make the back analysis very long or even impossible if numerical methods are implemented instead of the convergence-confinement method and on the other hand unique solutions are rarely obtained and depend on amount and type of uncertain parameters.

The so called Support Vector Machines (SVM) and numerical analysis with FEM and a Sequential Minimal Optimization (SMO) learning algorithm were developed by Xia-Ting et al. [3] for the Three Gorges Project in China. As written by the authors the SMO is a simple algorithm that can solve quadratic programming problems without any extra matrix storage and without using numerical quadratic programming optimization steps at all. This makes the computational requirements low, allowing the user to execute multiple calculations in a short period of time and to use the numerical analysis by the means of FEM only for verification purposes. This method is proposed for large projects where enough data is gathered for the genetic algorithms to evolve.

In [12] Zhang et al. use the three-dimensional finite element pattern technique (3-D FEPT) to analyze the measured displacements near the tunnel face. The model proposed by the authors is aimed on searching not more than two parameters, the

horizontal stress (P) and the Rock mass modulus (E). Taking this into account they implemented two techniques for the parameter's search. The first one is a direct search technique, where continuous search of P is done through DBBA and the parameter E is calculated from the final P estimation. The second is the damping least square technique, which compares the field measured displacements with those obtained from the DBBA. Back-analyzed results of E and P can then be optimized by minimizing the error function. Minimization requires a great amount of calculation by the 3-D FEM making the model time-consuming.

2. Inntal tunnel description

[13] The Inntal tunnel is one of the main components from the “Innsbruck freight railway bypass”. This bypass is a 14.8 km double-track electrified rail line, which connects the so called lower Inn tall railway with the Brenner railway, by-passing Innsbruck. It was opened on May 29th 1994 and has as major components:

- The Fritzens-Wattens 1 junction,
- A 488 meter-long bridge over the Inn river,
- The Innsbruck 1 junction and
- 12,696 meter-long Inntal tunnel.
    - Tunnel approx. costs €120 million to build

Photograph 1.: Inntal tunnel_Excavation in heavily squeezing rock[1]

[1] Photographer: Prof. DI Dr. Wulf Schubert

The Inntal tunnel is a two line tunnel between Inntal and Wipptal, its construction started in September 1989, by December 1992 the two excavation fronts broke through and the tunnel was completed in July 1993. After track laying, wiring of the overhead electrical line and the installation of signaling in the tunnel operations started in May 1994

The tunnel was built using the New Austrian Tunneling method. The distance between the tracks is 4.70 m, corresponding with high-speed lines and in contrast to other new tunnels, it is not built with slab tracks but instead is equipped with conventional ballasted tracks and concrete sleepers. The excavated cross-section goes from 95 to 108 square meters depending on the lining.

3. Parameters and data obtained in the tunnel

3.1. Analyzed cross sections

For the present master thesis a total of nine cross sections (see Fig. 2 and Table 1) were analyzed. The cross section selection was based on the final measured displacements and ground homogeneity. All analyzed cross section are modeled having a 113.1-m^2 cross section (6 m tunnel radius).

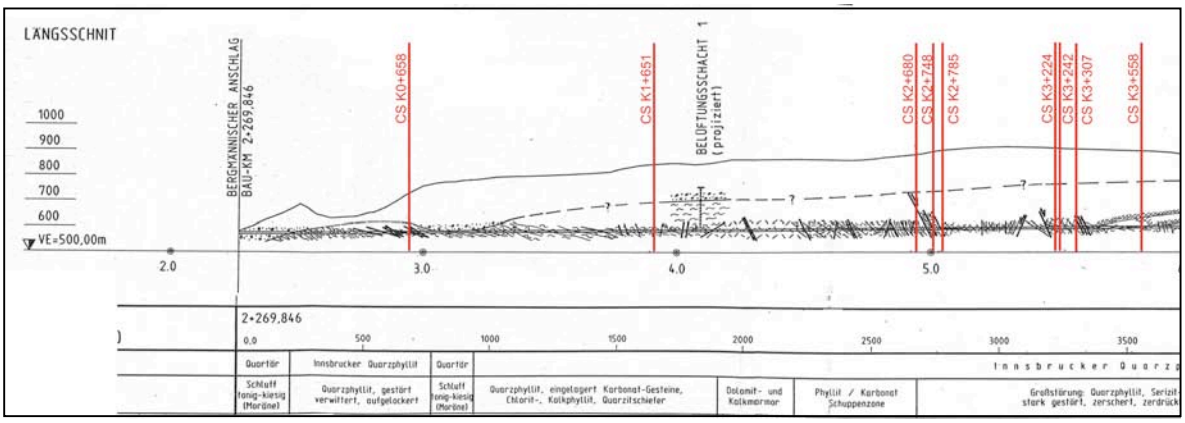

Fig. 2: Inntal tunnel longitudinal section

Csection	Geology
0+685	Quarzphyllite, disturbed, weathered, loose - low permeability - Foulted (mylonite)
1+651.4	Quarzphyllite, enbedded with carbonate rock, Chloritephyllite, limephyllite, schist quarzitte
2+680	Phyllite / carbonate rock scalezone
2+748	Masive Faults: Quarzphyllite, Serizitphyllite, Chloritphyllite, schist quarzitte disturbed, pulverized - brittle - partially plasticized - low permeability
2+785	
3+224	
3+242	
3+307	
3+558	

Table 1: Geological description from the analyzed cross sections

Although Kainrath et al. [14] recommend the convergence-confinement method for great depths and/or poor quality rock masses, the cross section 1+651.4 with relative low overburden inducing small displacements was analyzed for comparison reasons.

As written before the Inntal tunnel was constructed using the NATM, which assigns characteristic support systems based on rock mass behaviors along the tunnel axis. Therefore, often the same support system was found for more than one cross section. Table 2 presents the support systems installed in each cross section, Table 3 shows the properties for each support material.

				Shotcrete	Bolts				Steelribs (Profiles)	
Csection	**Displac.**	**Displac.(2)**	**Overburden**	**thickness**	**Type**	**long. Spacing**	**#Bolts**	**Length**	**Type**	**Steel. Spacing**
	(cm)	(cm)	(m)	(mm)		**(m)**		**(m)**		(m)
0+685	14.8	6.7	180-190	200	SN	1.5	9	3.9-6	HEA 120	1.5
1+651.4	7.6	3.2	340-350	200	SN	2.2	9	3.9-6	HEA 120	2.2
2+680	24.5	14.0	380	200	SN	1	10	6	HEA 120	1
2+748(1)	75.0	41.4	400	200	SN	1	29	8	Alpine	1
2+785(1)	58.6	33.8	410-420	200	SN	1	29	8-6.0B	Alpine	1
3+224(1)	81.2	57.8	405-415	200	SN	1	22	6.0-8.0	Alpine	1
3+242(1)	86.0	52.7	405-410	200	SN	1	22	6.0-8.0	Alpine	1
3+307(1)	69.5	41.9	395-405	200	SN	1	22	6	Alpine	1
3+558(1)	29.3	17.3	385-395	200	GEWI-SN	1	29	8-6.0B	Alpine	1

(1) Open displacement gaps

(2) Non time dependent displacements

Table 2: Installed support and registered displacements for the analysed cross section

Shotcrete					
Type	**Elasticity Modulus**			**Poisson**	
	(GPa)				
Wet	5 - 20.			0.25	
Steelribs (Profiles)					
Type	**Steel. Spacing**	**Flange width**	**Depth steel section**	**Cross-section area**	**Moment of inertia**
	(m)	(mm)	(mm)	(m2)	(m4)
HEA 120	1.5	120	114	2.53E-03	2.31E-06
Alpine	1	124	105.5	3.70E-03	6.16E-06
Bolts					
Type	**Bar. Diameter**	**Hole Diameter**	**E. Moduli Bar**	**E. Moduli Grout**	**Poison**	**Ultimate Load**
	(m)	(m)	(GPa)	(GPa)		(MN)
SN	0.025	0.052	210	25	0.15	0.3

Table 3: Support material properties

Displacements shown in Table 2 are the result of systematic measurements of the convergences for several days by means of electronic total stations and reflective targets. This system satisfies accuracy requirements and enables the evaluation of displacements in three-dimension. There are numerous ways for graphically displaying and interpreting the behavior along the tunnel surface. For this purpose the program Geofit, developed by 3G GRUPPE Geotechnik Graz was used. Fig. 3 shows a typical measured data analysis done by Geofit. The black dots represent the measured data on site and the blue and red lines are the fitted data for the top heading and bench respectively. The u_{eq} value (see Fig. 6) is represented by the end of the red line, where no further displacements are registered. Regarding the equilibrium point u_{eq} it is worth mentioning that time dependent displacements are not taken into account for the present study, for this reason only displacements up to 80m of distance to the face are considered.

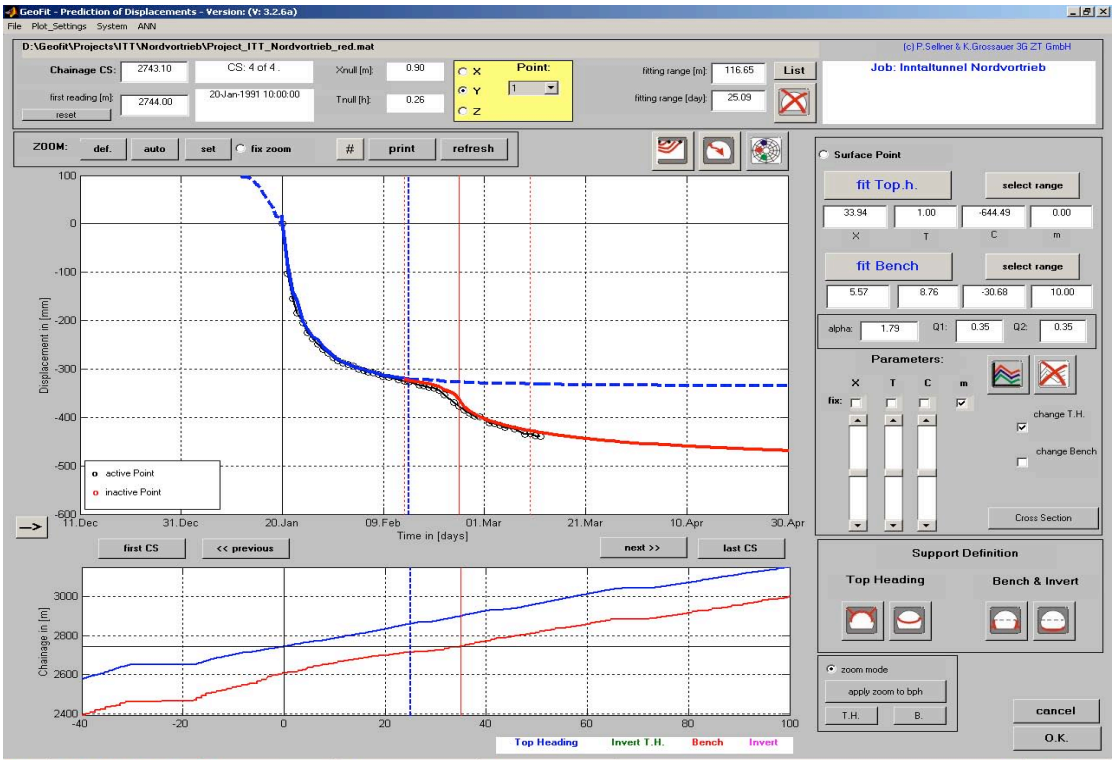

Fig. 3: Geofit scream shot, Software for displacement prediction_Cross section k2+743__Open gaps

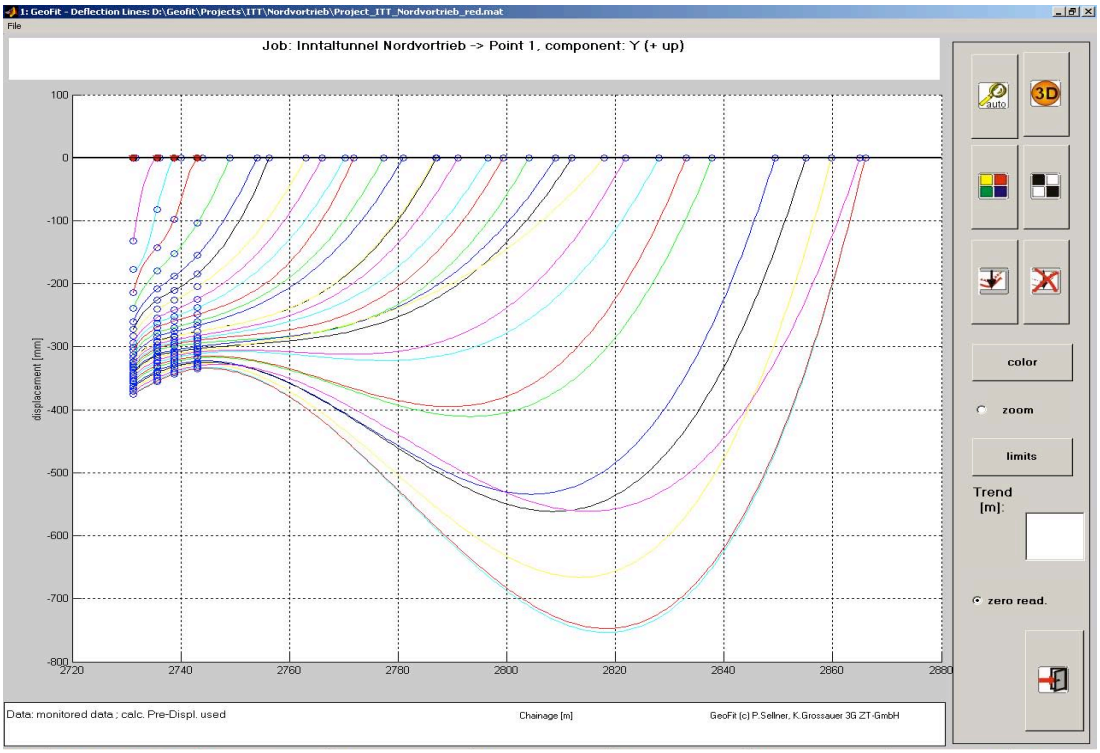

Fig. 4: Geofit Trendlines plot_Chainages K2+731.2 to K2+743.1

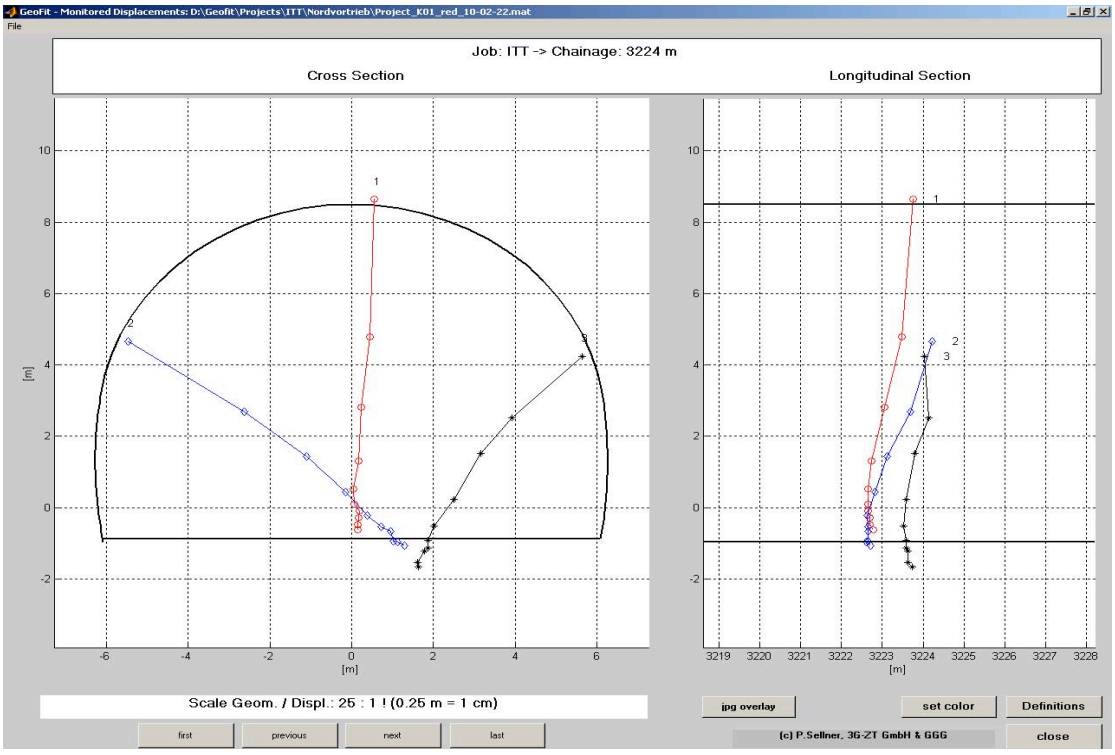

Fig. 5: Geofit's Cross- and Longitudinal-section_Cross section k3+224_open Gaps

Fig. 4 presents the development of the crown settlements between the chainages K2+731.2 and K2+743.1. Blue dots show the systematic measurements in the top heading for each cross section in between this chainages. The red path in Fig. 5 presents the crown displacements, which are used for the present study.

4. Proposed model for back analysis

4.1. Model overview

To carry out the back analysis, data regarding displacements and support system is necessary.

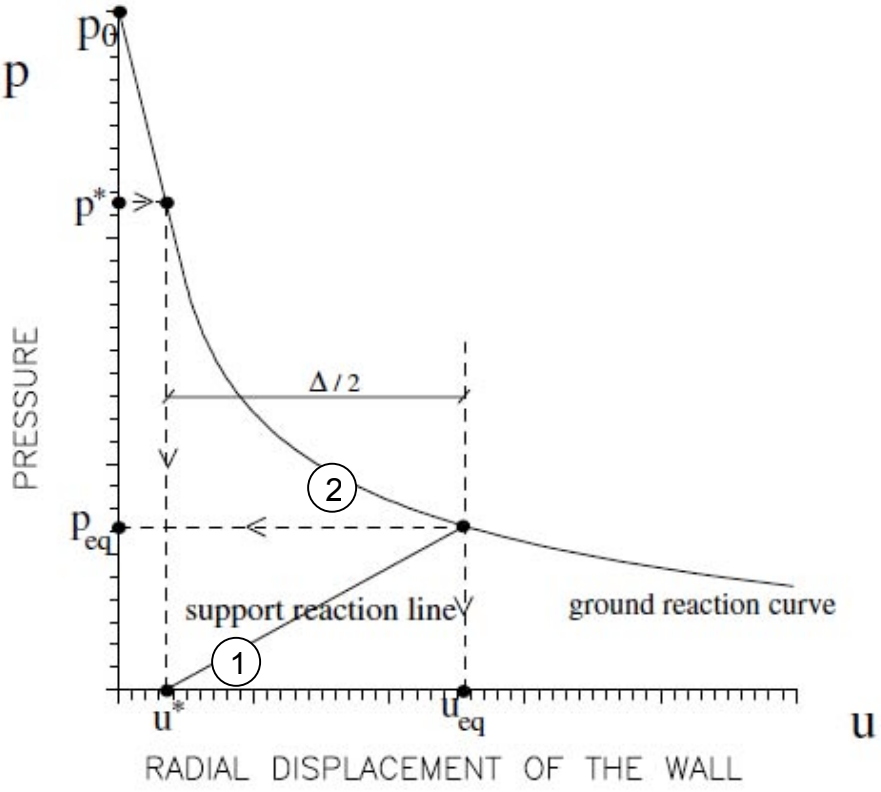

Fig. 6: Convergence-Confinement Method [5]

The proposed back analysis has the following procedure:

1) Determination of E_b, c_b, φ_b and E_t, c_t, φ_t

Where: the sub index b and t refer to bottom and top respectively and will limit the analysis range.

2) Determination of the GRC for E, c, φ according to Feder & Arwanitakis [1] formulation see curve 2 Fig. 6.

   Where: $E_1 = E_b$, $c_1 = c_b$ and $\varphi_1 = \varphi_b$ for the first analysis and,

   $E_n = E_t$, $c_n = c_t$ and $\varphi_n = \varphi_t$ for the last analysis

3) Calculation of pre-displacements after Hoek & Carranza-Torres [15] for the support installation (see u* in Fig. 6.)

4) Determination of the support characteristic curve (given by the support system installed) see curve 1 Fig. 6.

5) Determination of the equilibrium pressure point $u_{eq.}$ see Fig. 6.

6) Comparison between u_{eq} and the final measured displacements - Error calculation (R).

7) When the calculated error (R) is smaller than the admissible error (R_{adm}), the values of E, c and φ for the specific GRC are saved in a matrix.

8) The new input parameters are calculated as following:

   $E_i = E_{i-1} + E_{delta}$ and so on for c and φ values

   Delta is the increment value, calculated based on the partition given by the user.

9) The same procedure goes on until E_t, c_t and φ_t values are reached

The Flow chart from Fig. 7 summarizes the procedure.

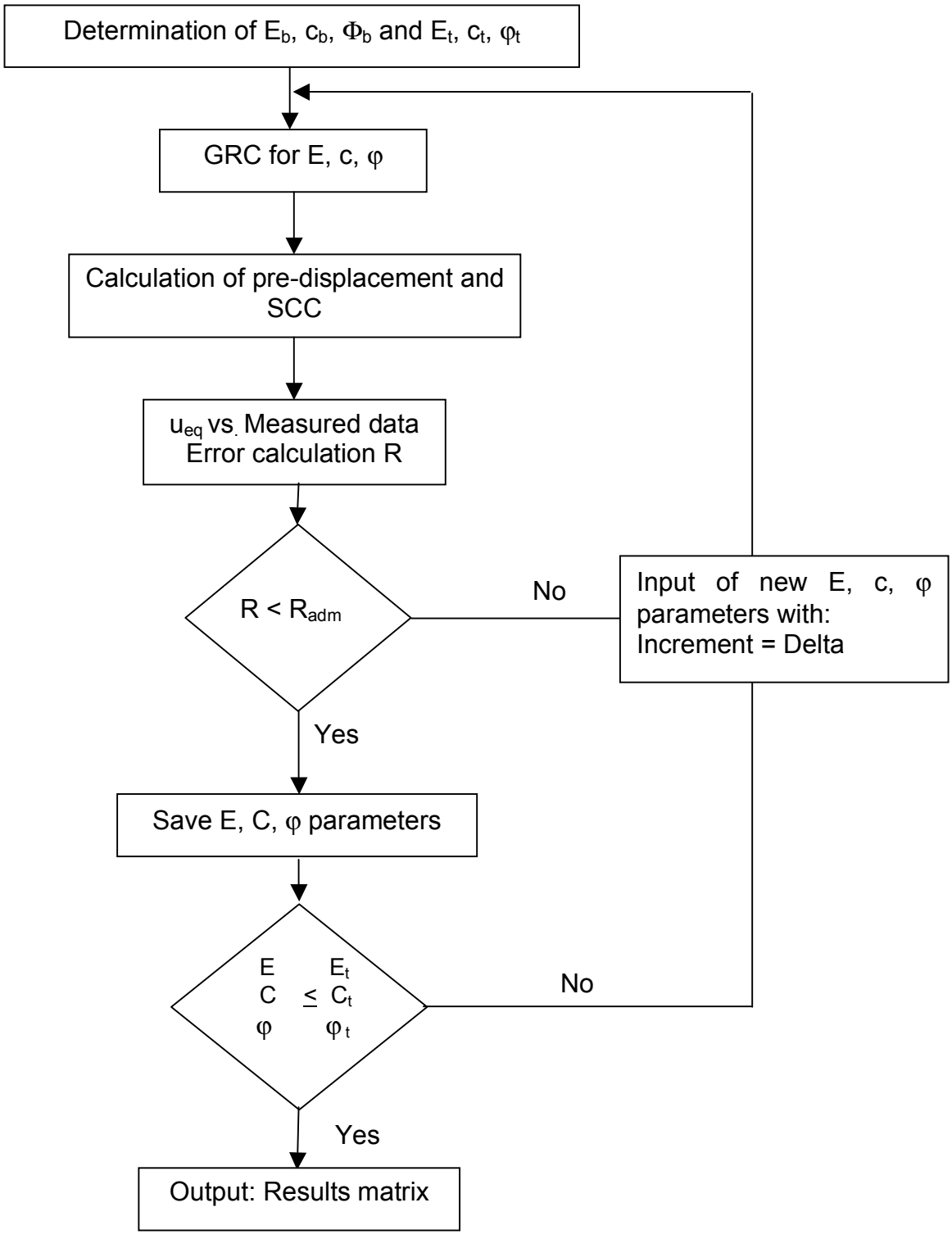

Fig. 7: Flow Chart Proposed Back Analysis

One has to be careful when making the initial assumption of E_b, c_b φ_b and E_t, c_t and φ_t hence they are not arbitrary values but rather have to be selected based on experience. This is due to the fact that mathematically speaking, it is possible to have combinations that fulfill the admissible error, but such combinations do not exist in most common rock masses.

It is worth mentioning that unlike [2], [3], [6], [9], [10] and [12] principal stresses are not calculated through back analysis but considered as known and estimated as a function of the overburden having K_0=1.

4.2. Model Basics

4.2.1. Ground Reaction curve (GRC)

The Convergence-Confinement method is a procedure that allows the calculation of the load imposed on a support installed behind the face of a tunnel. It is a practical tool but some considerations have to be taken into account. For the analytical solution delivered by the model used in the present study the following assumptions were made:

- 2D plate of infinite extend
- All deformations occur on a plane perpendicular to the tunnel axis
- Circular opening
- Homogeneous rock mass
- Side pressure coefficient K_0=1, (uniform stress field)
- No construction sequences
- Time-dependent weakening is not considered

The GRC was made according to the formulation from Feder & Arwanitakis [1]. In his research he stated that the final deformation for a circular tunnel has three different components: an elastic one, a plastic one and a volume increase in the plastic zone.

In the first part of Feder & Arwanitakis [1] present a formulation to mathematically describe the stress field for Mohr Coulomb material parameters, for a circular opening subjected to a uniform far-field (i.e. hydrostatic field) stress and uniform internal pressure, an example of this is shown in Fig. 8.

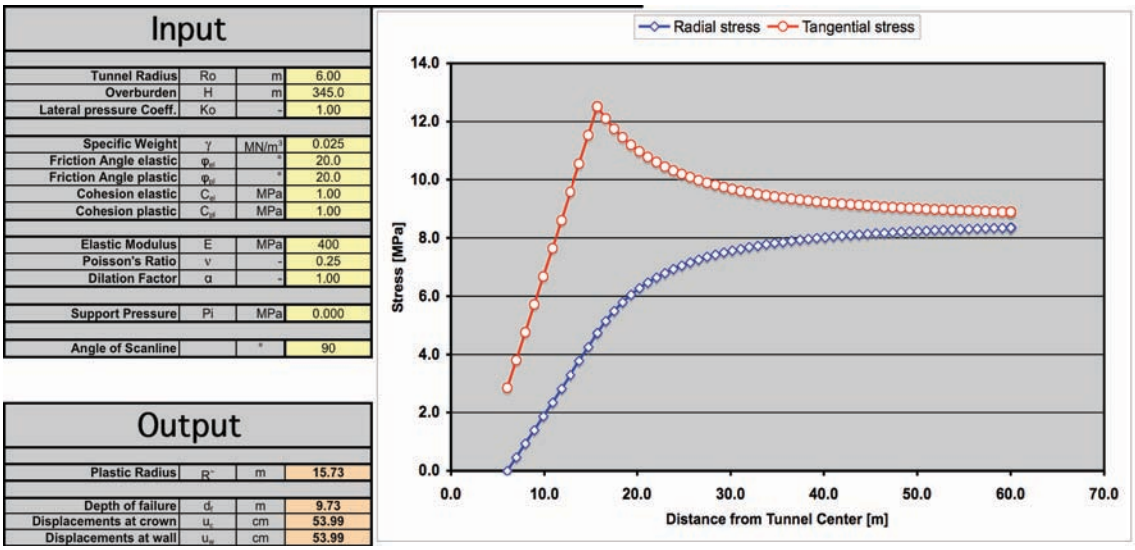

Fig. 8: Feder & Arwanitakis [1] stress field for a circular tunnel_K_o=1

In order to construct the GRC based on the formulation of Feder & Arwanitakis [1] one has to gradually change the inner support pressure P_i as follow:

1. Set $P_{i\_max} = \gamma * H = P_o$, as seen in Fig. 9 Model.

2. Gradually reduce the Internal pressure, up to a value P_{i_min}=0 (see Fig. 9. Step 2: No internal pressure), by doing this the analysis remains on the tunnel surface, as it is required for the GRC calculation. Analyzing equilibrium on one point of the tunnel intrado.

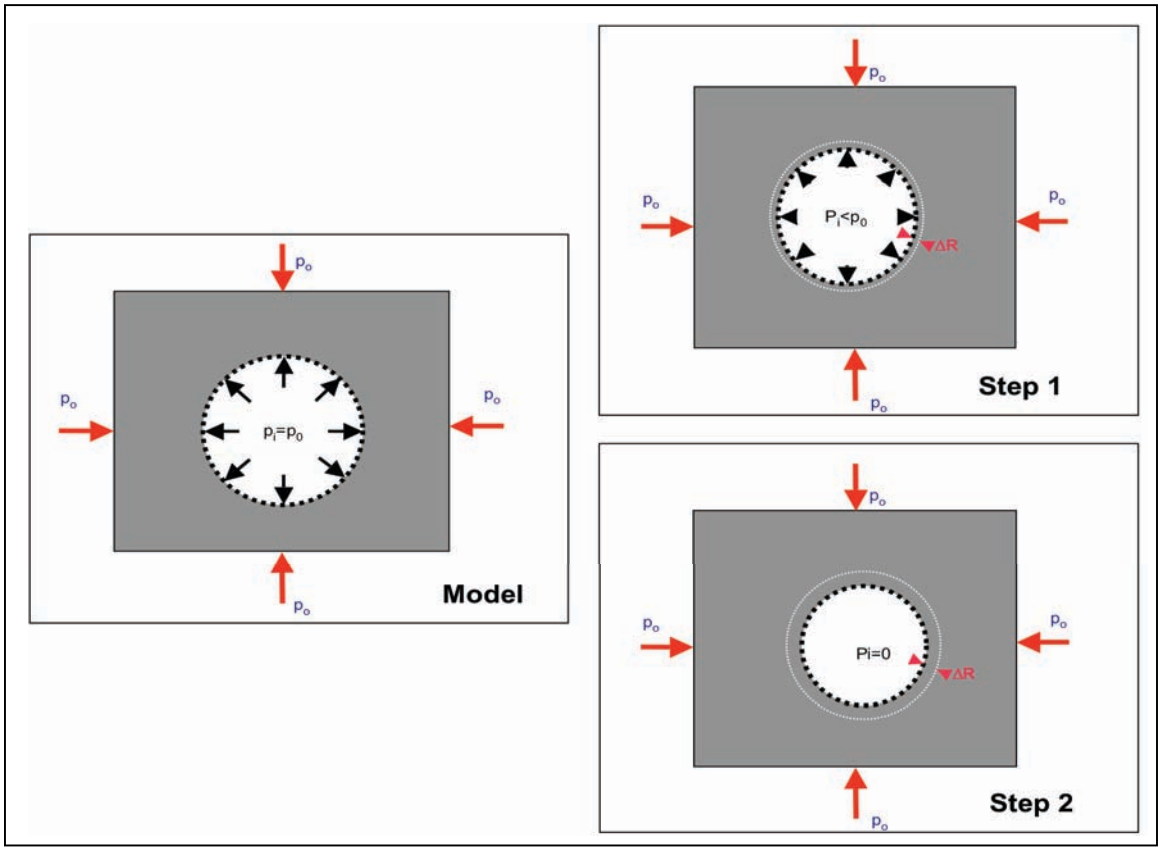

Fig. 9: GRC based on the formulation from Feder & Arwanitakis [1]

As explained before there are three main stress states in the formulation from Feder & Arwanitakis [1], for this reason for every P_i value a new Plastic radius has to be calculated and then the stress state verification can take place. Once the stress state is calculated the formulas for the specific scenario have to be implemented resulting on the given stress value P_i and a calculated displacement value *u*.

4.2.2. Ground Reaction Curve with improvement intervention

Improvement interventions refer to the use of grouted bolts, which themselves are not considered to establish any radial support pressure on the rock surface, therefore cannot be calculated as simple bars or cables. Forces in a grouted bolt have to be calculated depending on the rock mass deformation, these forces do not develop in a specific point but throughout the whole bar.

Authors have faced the problem by describing the bolt/ground interaction. For instance Indraratna and Kaiser in [16] and Oreste in [17] presented a solution based on a convergence control and the congruence of bolt-ground displacements respectively. Both authors modify the general elasto-plastic solution for the design of underground openings and extend it to accommodate the influence of bolt/ground interaction, size of opening and the bolt pattern on yielding and tunnel wall displacements.

For the present thesis expression (1) introduced in the literature by Grasso and Pelizza and mentioned by Oreste [17] was used. It shows the effect of the rock bolting on improving of the yielding zone around the tunnel in terms of effective cohesion.

$$c^* = c + \frac{1+\sin\varphi}{2\cos\varphi}\Delta\sigma_3 \tag{1}$$

where $\Delta\sigma_3$ is the confinement produced by the action of the grouted bolts, equal:

$$\Delta\sigma_3 = \frac{T_m}{S_T + S_L} \tag{2}$$

where T_m is the mean force along each bolt, S_T and S_L are transversal and longitudinal spacing of the bolting pattern.

The mean force value was calculated using the finite difference calculation procedure proposed by Oreste [17]. Oreste's method is divided in 7 main steps:

1. Setting out a value of $|t_B|$ (shear stress between the bolt and the rock in the anchorage zone. $|t_B|$ is calculated based on the T_0 value which is the discharge of the bolt onto the tunnel walls and the T_{max} value which is the Maximum traction force in the bolt that will later be recalculated.

2. Determination of the circumferential stress and of the radial displacement in each point of the bolt (at a known distance from the centre of the tunnel) with variation of radial stress in the same point

3. Calculation of stresses and strains in the reinforced rock, until the group of values from circumferential stress, radial displacement and plastic radius is calculated for each term

4. Selection of the group of values for which the circumferential stress is more approximated to the given internal pressure of the tunnel perimeter

5. Determination of stresses and displacements in the reinforced rock for the distance R_i

6. Congruence verification between the deformation of the rock and the deformation of the bolt

7. Estimation of the T_{max} value

Once the T_{max} value is calculated for the found shear stress $|t_B|$ the T_{mean} value can be calculated by means of expression (3):

$$T_{mean} = \frac{T_{\max}}{2}\left[1 + \chi\left(\frac{1}{2} - \frac{\eta}{L}\right)\right] \tag{3}$$

where η is the distance of the location of the maximum force from the median point of the bolt and χ is the ratio between T_0 and T_{max}, from the numerical modeling presented by Oreste [17], one can conclude that η and χ vary in a narrow interval, and the mean values $\eta=1/3$L (where L is the length of the bolt) and $\chi=1/3$ can be taken when a perfect constrain is obtained on the bolt head.

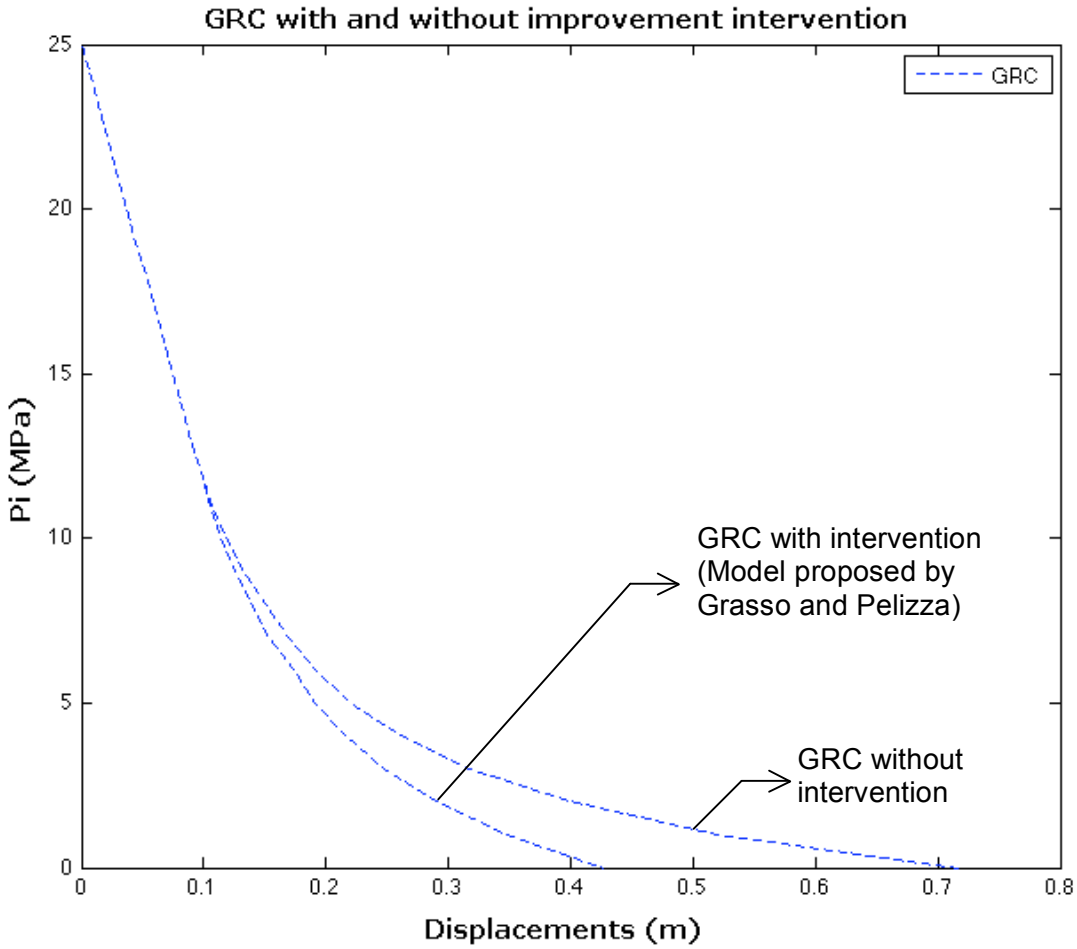

Fig 10: **Ground reaction curve with and without improvement intervention after Oreste [17]**

Fig. 10 shows Oreste's approach implemented in Matlab and an example of the ground reaction curve modification

There are two main remarks from Fig. 10:

1. Since it is assumed that by the time the bolts are installed elastic displacements have taken place, it is visible that the GRC modification only occurs in the plastic zone.

2. The original formulation made by Oreste in [17] had to be modified. The reason for that was the great reduction of displacements. Several calculations were made and it could be seen that, when significant displacements are taking place (i.e., Displacements in Inntal tunnel) the original formulation overestimates ground conditions. Through the calculations one could notice that the tensile force T_{max} in each bolt was not limited carrying out the mentioned overestimation. The problem was easily fixed by establishing a max. tensile load of 300 kN. The mentioned value was selected taking into account the diameter and type of bolts used in the Inntal tunnel.

4.2.3. Support Characteristic Curve

The principles of the SCC are well explained by Carranza & Fairhurst in [18] and by Stille et al. in [19] the original formulation has Hoek & Brown (1980) and Brady & Brown (1985) as authors. The principle for the construction of the SCC is based on the elastic relationship between the applied stress P_s and the resulting closure u_r for a unit length section of the support in the direction of the tunnel (longitudinal spacing). An elastic stiffness of the support "K_s" ought to be determined. The elastic part see curve 1 Fig. 6 of the SCC can be calculated after the following expression:

$$P_s = K_s * u_r \quad (4)$$

The plastic part of the SCC is defined by the maximum pressure P that the specific support system can bear before collapse.

4.2.3.1. Shotcrete or concrete rings

Considering the closed ring of shotcrete or concrete represented in Figure 11, the maximum pressure provided by the support is:

$$p_s^{\max} = \frac{\sigma_{cc}}{2}\left[1 - \frac{\left(R - t_c\right)^2}{R^2}\right] \tag{5}$$

The elastic stiffness is:

$$K_s = \frac{E_c}{\left(1 - \upsilon_c\right)R}\left[\frac{R^2 - \left(R - t_c\right)^2}{\left(1 - 2\upsilon_c\right)R^2 + \left(R - t_c\right)^2}\right] \tag{6}$$

where:

σ_{cc} is the unconfined compressive strength of the shotcrete or concrete [MPa];

E_c is Young's Modulus for the shotcrete or concrete [MPa];

υ_c is Poisson's ratio for the shotcrete or concrete;

t_c is the thickness of the ring/shotcrete [m];

R is the external radius of the support [m]

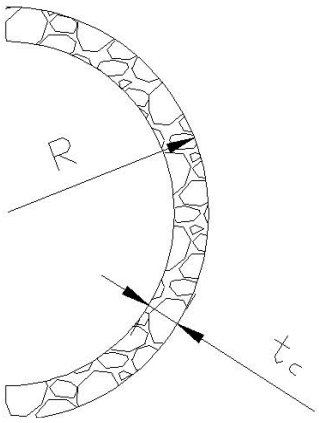

Fig. 11: Schematic representation of sections of shotcrete/concrete rings adapted from Brady and Brown (1983).

4.2.3.2. Steel profile sets

Regarding the Steel profiles a change had to be carried out due to the fact that the formulas presented by the authors supposed, that the profiles are tightened against the rock by using wood blocks, which is a common practice in North and Latin America. Common practice in Europe is to set the profiles directly against the shotcrete. Comparison between wood blocks and shotcrete were evaluated and the conclusion is that the contribution from the wood blocks in terms of maximum pressure is too low. Therefore the part of the equation where block sets are considered does not form part of the present study.

Considering steel sets spaced a unit length apart in the direction of the tunnel axis and tightened against the rock by shotcrete the maximum pressure that the system can sustain is:

$$p_s^{\max} = \frac{3}{2}\frac{\sigma_{ys}}{S\,R} + \frac{A_s I_s}{3I_s + D\,A_s[R - 0.5D]} \tag{7}$$

The elastic stiffness is:

$$K_s = \frac{E_s A_s}{S_c R^2} \tag{8}$$

Where:

- B is the flange width of the steel set [m];
- D is the depth of the steel section [m];
- A_s is the cross-sectional area of the section [m^2];
- I_s is the moment of inertia of the section [m^4];
- E_s is Young's modulus for the steel [MPa];
- σ_{ys} is the yield strength of the steel [MPa];

S is the steel set spacing along the tunnel axis [m];

R is the tunnel radius [m].

4.2.3.3. Ungrouted bolts and cables

The sketches in Fig. 12 represent mechanically anchored bolts installed in the rock-mass surrounding a circular tunnel of radius R. Assuming that the bolts are equally spaced in the circumferential direction, the maximum support pressure provided by this support system is:

$$p_s^{\max} = \frac{T_{bf}}{S_c + S_l} \tag{9}$$

The stiffness is:

$$\frac{1}{K_s} = S_c S_l \left[\frac{4l}{\pi\, d_b^2 E_s} + Q \right] \tag{10}$$

Where:

d_b is the bolt or cable diameter [m];

l is the free length of the bolt or cable [m];

T_{bf} is the ultimate load obtained from a pull-out test [MN];

Q is a deformation-load constant for the anchor and head [m/MN];

E_s is Young's Modulus for the bolt or cable [MPa];

S_c is the circumferential bolt spacing [m];

S_l is the longitudinal bolt spacing [m].

The equation presented for the non grouted bolts supposes that the reaction forces developed by the bolt are concentrated at the ends of the bar; therefore the equation should not be applied in the case of grouted bolts, for which the load transfer is distributed throughout the length of the shank.

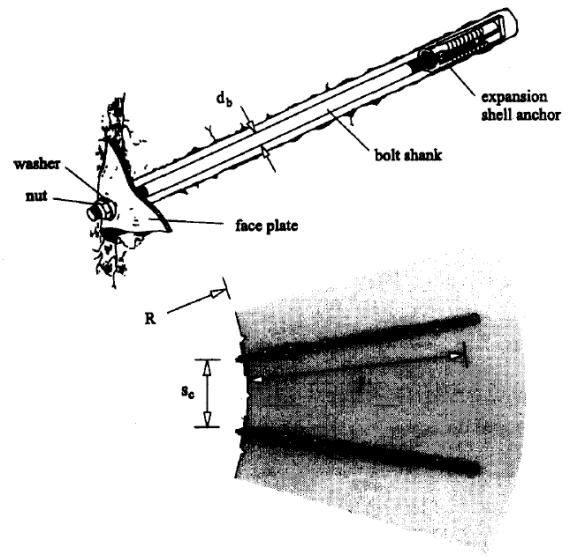

Fig. 12: Ungrouted mechanical-anchored bolt (adapted from Stillborg 1994 and Hoek and Brown 1980).

4.2.3.4. Lining stress controllers

[20] The SCC for integrating yielding elements can be approximated by a bi-linear relationship (or as a combination of bi-linear relationships). The initial branch of resistance mobilization is of great importance since the young shotcrete still has a very low strength. The mobilized support resistance P_A in this phase can be derived with Equation 11.

$$p_A = \frac{2u_{Ausbau}\pi}{R\left[\frac{2R\pi - n_{St}l_{St}}{E_{SpB}t_{SpB}} + \frac{n_{St}}{K_{St}}\right]} \tag{11}$$

where:

u_{Ausbau} is the radial displacement of the support [m];

n_{St} is the number of yielding elements in the cross section;

l_{St} is the length of the yielding element gap in the shotcrete lining [m];
E_{SpB} is the secant Young's modulus of the young shotcrete [MPa];
t_{SpB} is the thickness of the shotcrete shell [m];
K_{St} is the initial stiffness of the yielding element [kN/m];
R is the tunnel radius [m].

As recommended by [20] Radoncic, Schubert and Moritz, a secant Young's modulus of 5,000 MPa should be assumed, since the relationship shown in Equation 11 would give unsafe results if the shotcrete stiffness was assessed too low. The radial displacement at which the yielding occurs is calculated as following (Equation 12):

$$u_{pl} = u_0 + \frac{1}{2\pi}\left[\Delta l_{pl} n_{St} + \frac{F_{pl}}{E_{SpB} t_{SpB}}\left(2R\pi - l_{St} n_{St}\right)\right] \tag{12}$$

where

F_{pl} is the force in the yielding element when the yield is reached [kN];
u_{pl} is the shortening when the yield is reached [m];

The support resistance mobilized in this phase is calculated from the yield load of the elements (Equation 13).

$$P_{A,pl} = \frac{F_{pl}}{R} \tag{13}$$

Most yielding elements feature a second increase in the mobilized loads after a certain compressive displacement Δl_{AN} is reached. By using simple geometrical considerations, the radial displacement u_{AN}, at which the support resistance curve starts to increase again, can be calculated through equation 14.

$$u_{AN} = u_0 + \frac{\Delta l_{AN} 2\pi}{n_{St}} \tag{14}$$

Since the shotcrete is already cured at this moment, the compressive strain increments in this phase can be neglected. Thus, the support resistance can be calculated in a straightforward manner, and added to the already mobilized resistance from the plastic phase by means of equation 15.

$$p = p_{A,pl} + \frac{(u_{Ausbau} - u_{AN}) K_{St,AN}}{n_{St}} \tag{15}$$

where:

$K_{St,AN}$ is the stiffness of the yielding element in the phase of load increase.

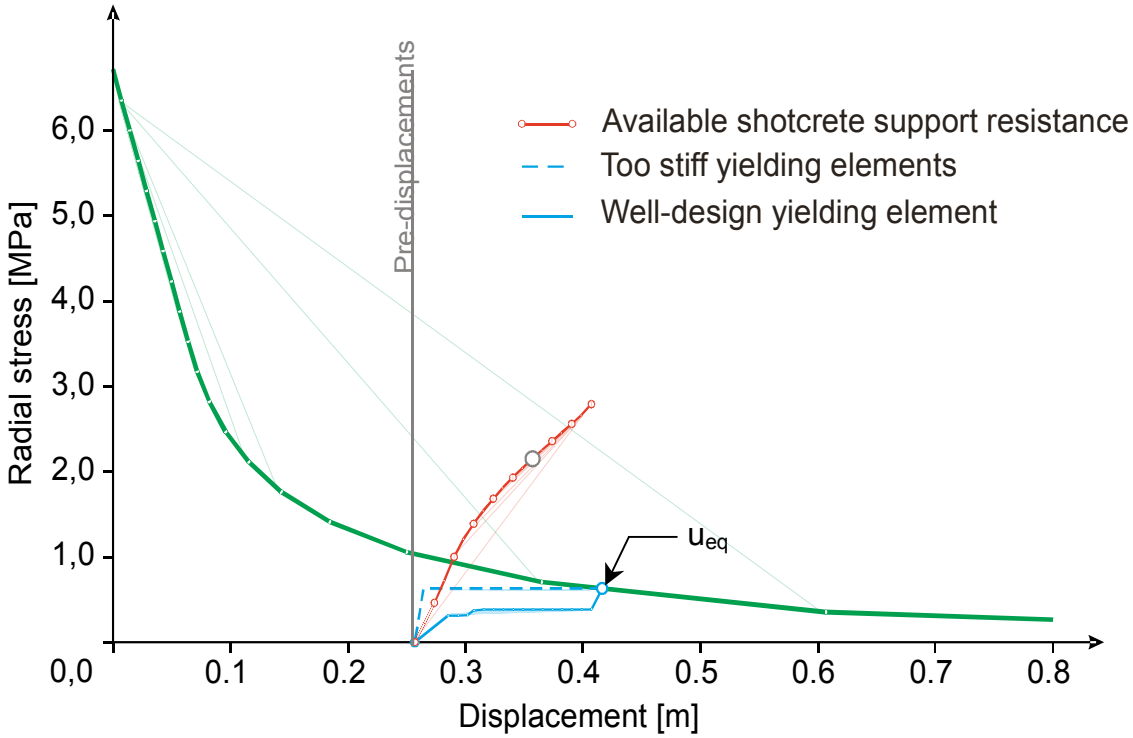

Fig. 13: GRC and SCC for Lining Stress Controllers_Taken from [20]

The equilibrium displacement u_{eq} (see Fig. 13) is given by intersecting the ground convergence curve with the support resistance curve obtained by applying the equations above.

4.2.4. Pre-displacement calculation

Hoek et al. in [21] and Carranza & Fairhurst in [18] presented Hoek's empirical best-fit relationship between radial displacements of the tunnel and distance to the face (see expression 16). Hoek's empirical approach was based on convergence measurements made in the Mingtam Power Cavern project by Chern et al. (1998), these measurements were fitted into the following equation:

$$\frac{u_r}{u_r^M} = \left[1 + e\left(-\frac{x/R}{1.10} \right)^{-1.7} \right] \tag{16}$$

where:

- x is the distance to the tunnel face [m];
- u_r^M is the maximal radial displacement [m];
- R is the tunnel radius [m];
- u_r is the predicted displacement [m].

Based on Hoek's equation Carranza and Fairhurst made the following observations:

- The maximum radial displacement occurs at approximately 8 tunnel radii behind the face of the tunnel.
- The radial deformation is zero at approximately 4 tunnel radii ahead of the face.
- At the face itself, the radial displacement is approximately 30% of the maximum displacement value.

4.3. Model Shortcomings

4.3.1. Ground Reaction Curve and Support Characteristic Curve

For the GRC construction the present study considers rock masses that satisfy Mohr Coulomb failure criteria, only peak values from E, c and φ are handled, post failure behavior is not considered.

The SCC in the model does not consider installation time and excavation sequences, it is assumed that the used support system for each cross section is installed at the same time. It is worth mentioning that minor changes have to be made in order to take these considerations into account, but due to the lack of information regarding installation timing this assumption was necessary.

The plastic part of the SCC in Figure 6 i.e., the horizontal segment, is defined by the maximum pressure that the support can accept before collapse, no post-failure consideration was made for the materials used as support.

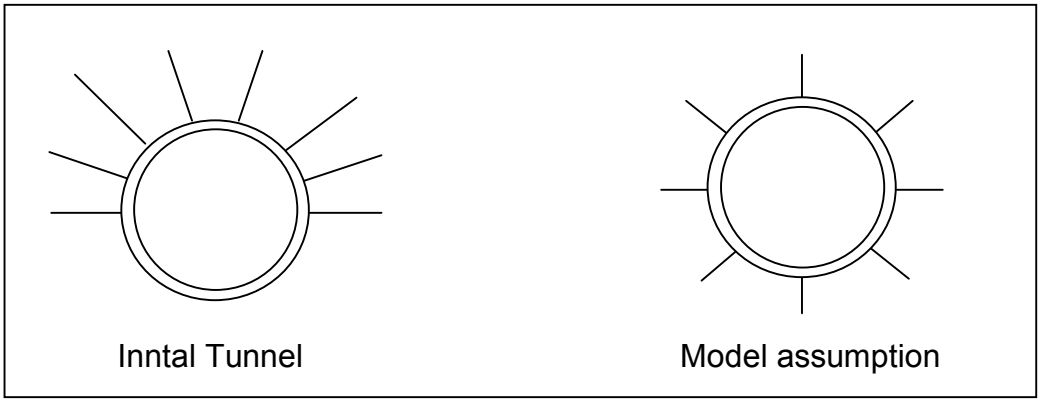

Fig. 14: Bolting distribution found on site and for the proposed model

The time dependency of shotcrete in terms of strength is not included in the present model. Shotcrete is always considered as “young”. Therefore values in between 5 and 10 MPa were handled.

Bolting distribution in each cross section is assumed to be equidistant and bolts to have the same length. Fig. 14 shows an example of a bolting system (8 bolts) on a cross section.

Bolts installation is assumed to occur after elastic displacements have taken place, as seen in Fig. 10 the GRC is only modified on its plastic part.

As described in the introduction the presented model allows the user to select a range of Young’s modulus, cohesion and friction angles where the back analysis will take place. However these values have to be determined by the user based on experience, since it is possible to find combinations that are mathematically correct but are rarely found in rock masses.

4.3.2. Dilatancy

Dilatancy is a major shortcoming of the presented model. As described by Alejano and Alonso in [22] difficulties associated “with a model that adequately reflects observed complete stress–strain curves have affected the possibilities of developing suitably valid approaches for handling post-failure strength behavior and dilatancy”, this mainly happens because problems in rock mechanics avoid failure and the inherent difficulty of calculating dilatancy.

The formulation from Feder & Arwanitakis [1] does not take into account dilatancy. Due to the fact that it plays an important role in rock mechanics where shear strains occur (i.e. along fault zones and discontinuities) further studies should be made regarding this matter. Setting dilatancy into the model would imply a change

in the whole GRC since dilatancy develops only as the deformation (displacements) process unfolds.

Further studies ought to be done regarding dilatancy influence on the grouted bolts behavior. For the present study dilatancy was set (ψ=0), Oreste in [17] remarked dilatancy mayor role in the bolts performance since it only fully unfolds in a post-failure rock state.

4.3.3. Consideration for the Inntal tunnel

A final consideration had to be made in order to handle the support design made for the Inntal tunnel where heavily squeezing rock was found. The support design in those areas involved the usage of the so called open displacement gaps as seen in Photograph 1. The model modification for this scenario was divided in two parts:

1. **Shotcrete contribution ratio:** Though, Pöttler in [23] carry out a study on shotcrete contribution by presence of open gaps, this approach was not included in the present study, mainly because parameters describing the interaction ground-shotcrete are not available. Nevertheless a simulation was performed on the program Phase^2, developed by RocScience in order to find a shotcrete contribution ratio, which allows inferring the open gaps by minimizing the parameters of the closed shotcrete ring.

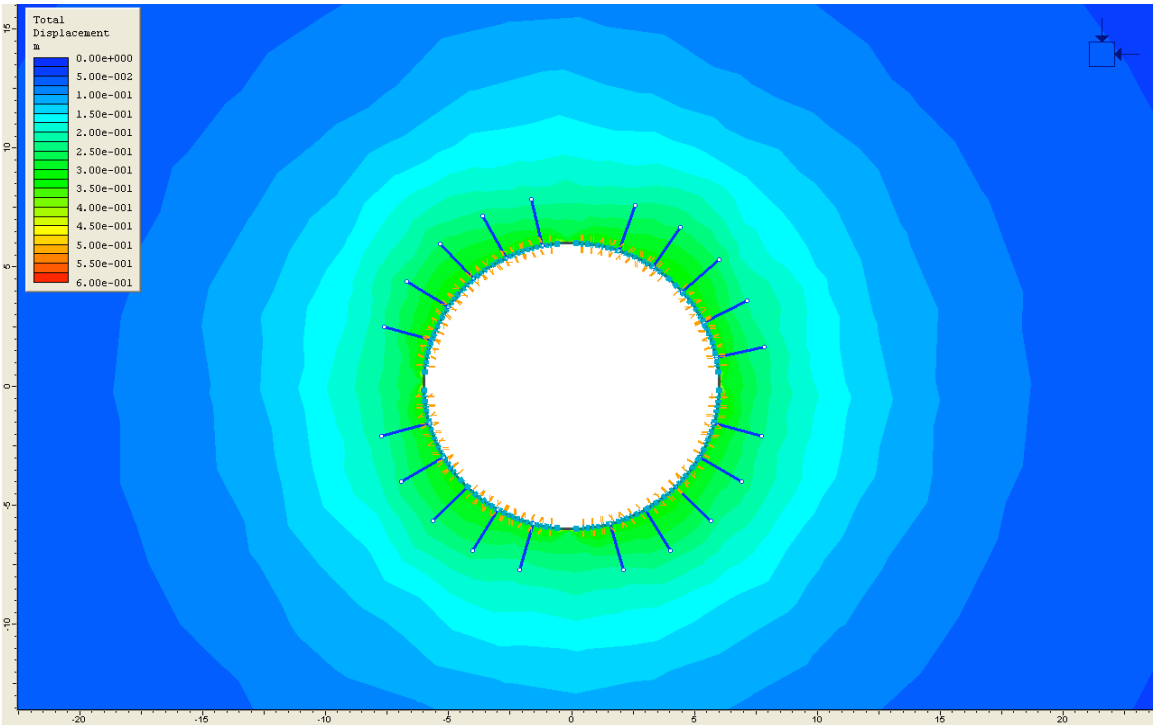

Fig. 15: Phase^2 displacements prediction_Cross section with open gaps

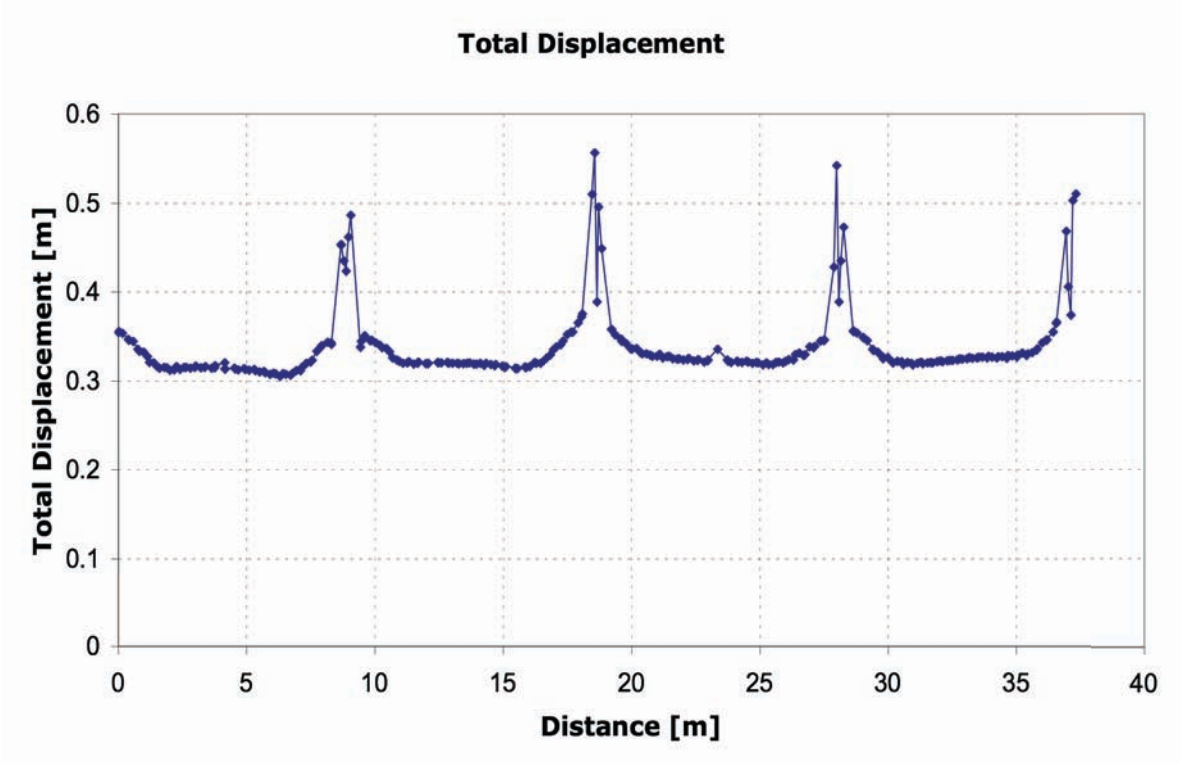

Fig. 16: Phase^2 displacements prediction_Cross section with open gaps along unbound cross section

Fig. 15 and Fig. 16 show the total displacements delivered by Phase[2]. In order to find the concrete contribution ratio, two scenarios were calculated and compared in terms of the internal pressure delivered by the shotcrete[1], one with the open gaps and one without them. A ratio was calculated by means of equation 17.

$$\text{Shotcrete contribution ratio} = \frac{\text{Support pressure with open gaps}}{\text{Support pressure without gaps}} \times 100 \quad (17)$$

The output of that simulation was a ratio of 10% of the support pressure delivered by the shotcrete under normal condition, when using the open displacement gaps. (See Fig. 16)

2. **Open gaps closure:** the open gaps aperture for a given cross section is taken as an input value, which allows the model to estimate the distance to the face in which the open gap closes, once the gap closes the system acts as a closed-ring, as seen in Fig. 17 (red line) there is a load increment starting in the point where the gaps close. It is assumed that the tunnel closes in radial direction at a constant rate.

[1] Data taken from phase[2] refer to displacements values, which had to be transferred into Feder's worksheet (see Fig. 8) in order to calculate the internal pressure P_i (see Fig. 9) needed to reach this displacement value.

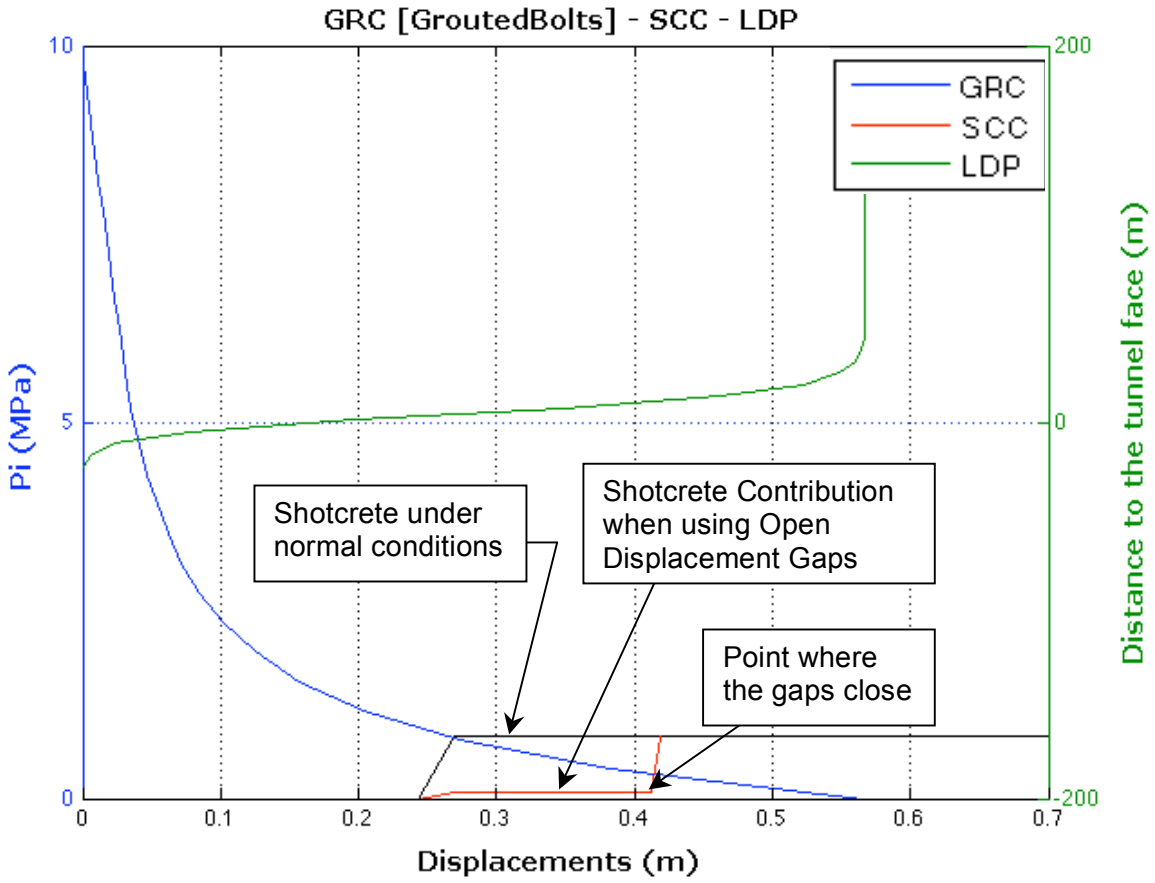

Fig. 17: Shotcrete contribution for support systems with open gaps

5. Results

5.1. Back analyzed parameters

Table 4 shows the input parameters and the limit values for E, c and φ for each analysis. Table 5 summarizes the back-analyzed parameters with the minimum, maximum and mean value for each parameter in each one of the nine cross sections.

Cross Section	Overburden	Messured Displa.	Back analysis limits					
			E_min	E_max	c_min	c_max	Phi_min	Phi_max
	[m]	[m]	MPa		MPa		[°]	
0+685	190	0.095	500	4500	0.1	2.1	20	30
K1+651	345	0.048	800	7800	0.1	3.6	20	40
k2+680	380	0.199	500	6500	0.5	3.5	20	35
k2+748	400	0.564	300	1800	0.1	1.6	15	22.5
k2+785	415	0.445	300	1300	0.1	1.6	15	22.5
k3+224	410	0.704	300	1800	0.1	1.6	15	22.5
K3+242	410	0.659	300	1800	0.1	1.6	15	22.5
k3+307	400	0.574	300	1800	0.1	1.6	15	22.5
k3+558	390	0.227	300	2300	0.1	2.1	15	25

Table 4: Summary Back-analyzed limits for the Inntal Tunnel

Analysis limits shown in Table 4 were chosen in order to calibrate the model. Through this process the need of expertise for the selection of such limits is noticed.

Cross Section	Overburden	Messured Displa.	Backed Analized parameters								
			E_min	E_max	E_mean	c_min	c_max	c_mean	Phi_min	Phi_max	Phi_mean
	[m]	[m]	MPa			MPa			[°]		
0+685	190	0.095	500	2500	1194	0.1	0.8	0.34	15	29.5	20.6
K1+651	345	0.048	1400	6600	2508	0.1	3.6	1.52	20	40	28.9
k2+680	380	0.199	500	2900	916	0.2	1.7	0.73	20	35	26.2
k2+748	400	0.564	300	1800	938	0.1	1.3	0.53	15	22.5	18.3
k2+785	415	0.445	300	1800	874	0.2	1.6	0.81	15	22.5	18.6
k3+224	410	0.704	300	1800	794	0.2	1.4	0.68	15	22.5	18.4
K3+242	410	0.659	300	1800	865	0.2	1.5	0.68	15	22	18.5
k3+307	400	0.574	300	1800	863	0.2	1.6	0.76	15	22.5	18.9
k3+558	390	0.227	500	2300	1207	0.3	2.1	1.06	15	25	20.1

Table 5: Summary Back-analyzed values for the Inntal Tunnel

The mean values seen in Table 5 have to be handled with carefulness, since they only depend on the limits chosen for the analysis. Regarding Table 5 it is important to emphasize the back-analyzed cohesion values. They move in a rather small range compared to the E and φ values. It was also observed that the cohesion upper limit is fixed, regardless of the E and φ. This behavior is not seen for φ, which are clearly related to the Young's modulus.

Fig. 18 and 19 graphically summarize the back-analyzed parameters for the cross section k1+651 and k3+307 respectively. As expected for high Young's moduli, lower c and φ parameters are needed in order to accomplish the same displacement values u_{eq} (see Fig. 6), this trend is seen in all the back-analyzed cross sections. A linear trend is also observed in these figures for each Young's modulus. This was also expected, since the formulations used for the present thesis describe rock masses with linearly elastic - ideally plastic material behaviour.

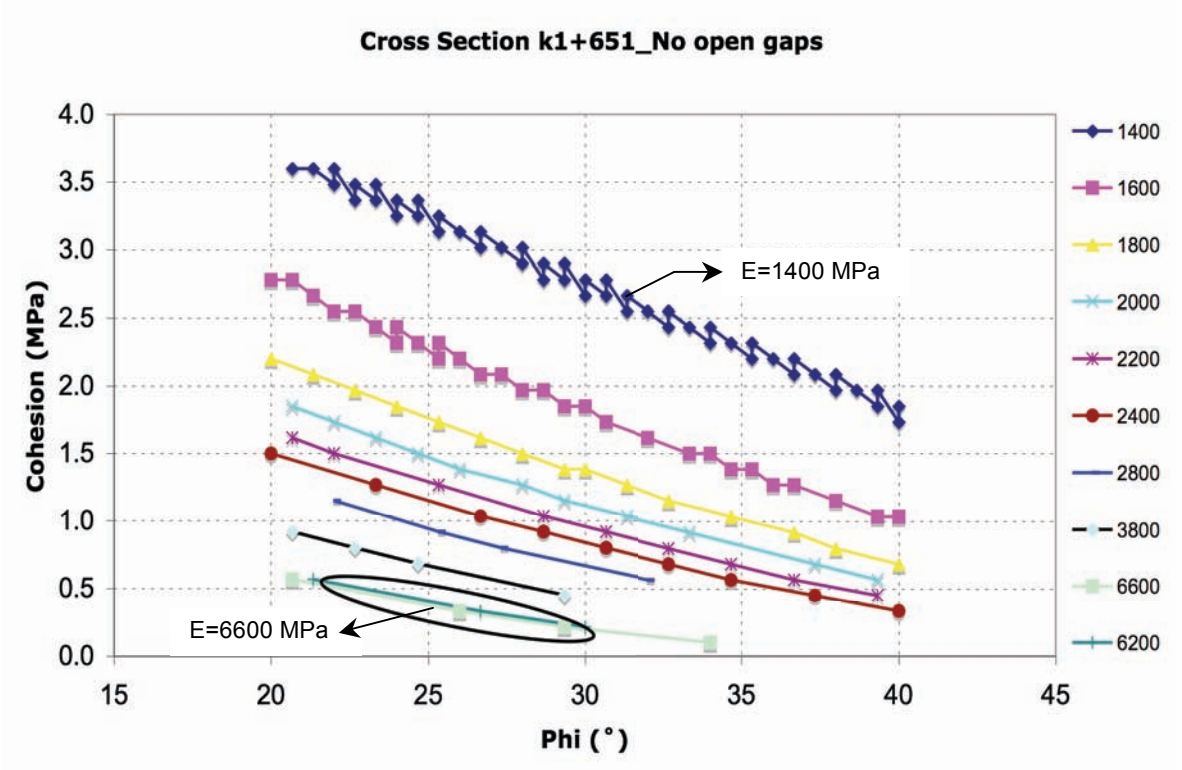

Fig. 18: Results Cross section K 1+651_No open gaps

The limits selection for the back analysis was made based on experience. It is noticed that the value used for the cross section without open displacement gaps are significantly higher than those chosen for the cross section without them, this was made in order to be in agreement with the observed displacement values.

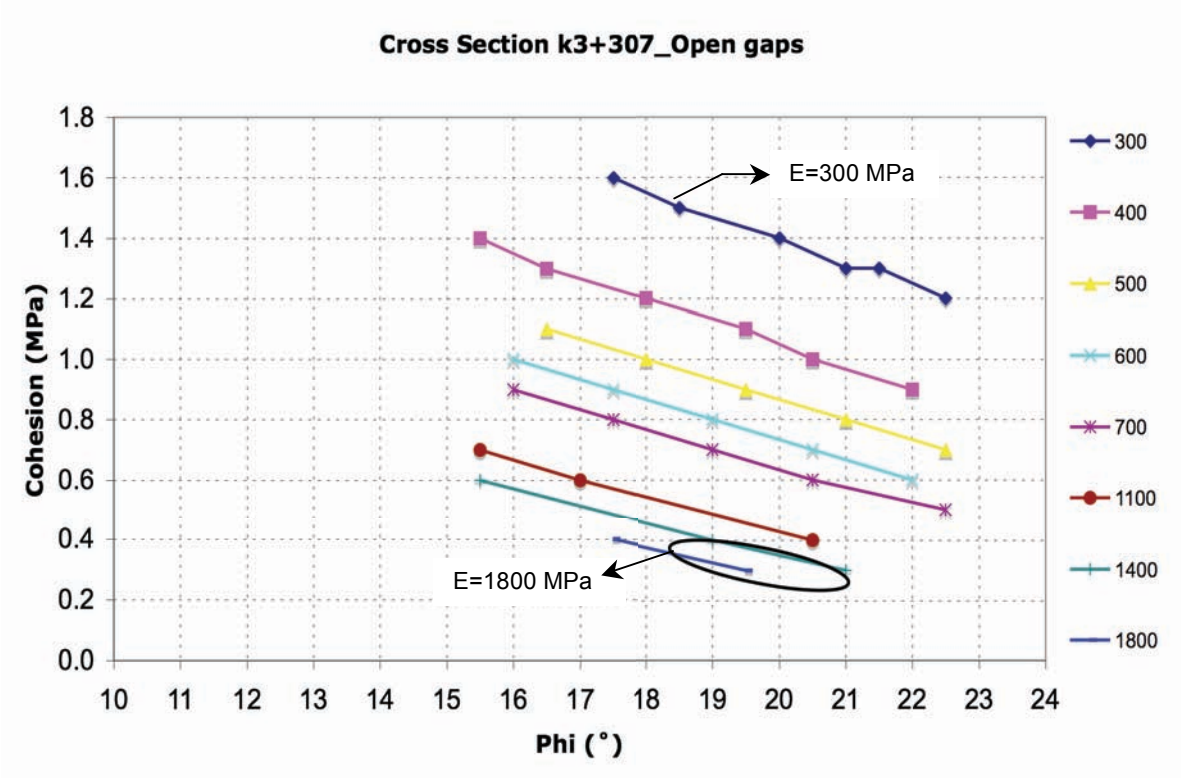

Fig. 19: Results Cross section K 3+307_Open gaps

5.2. E, c and φ range selection

As written before, the results of the back analysis itself delivered a wide range of values that fulfill the measured displacements, in an attempt to reduce this range two different approaches were implemented into the model: Axisymmetric modelling and convergence analysis from Panet & Guenot formulation [24].

5.2.1. Axisymmetric modeling

Using the FE computational program Phase^2 one can simulate an advance rate and its influence on the displacements for a given cross section. Fig. 20 and 21 show the models assembled for the cross section k0+685 and k2+748 respectively. For each cross section a model was made considering the following points:

- **Distance to the face of min. 80m**: this distance was selected, based on the measured displacements, in order not to take into account time dependent displacements. Each model was divided into stages simulating the excavation rate given by the design.

- **Support systems**: Axisymmetric models in Phase^2 do not allow the user to implemented a support system itself, but rather simulate it as an internal pressure value “Pi”, The internal pressure value was calculated for each cross section based on the support design and implemented into the model as the excavation stages were taking place (See excavation red arrows Fig. 20)

- **Open displacement gaps:** For the cross section with open displacements gaps a special consideration was made regarding the support system since the gaps have a max. closure distance. With the help of the longitudinal deformation profile (LDP) it was possible to establish the distance to the tunnel face in which this closure takes place and from that point on set a higher internal pressure “Pi” representing the closed shotcrete lining (see Fig. 21).

- **Displacement development:** As explained in chapter 3. displacement data was measured using reflective targets located at a know cross section, the same principle was implemented in the Phase^2 model, one point was defined in order to estimate the displacement development related to advance excavation (see point “A” Fig. 20).

Fig. 22 shows the displacements results for point “A”, this example is the simulation in cross section 2+785_Open gaps, where each stage simulates an excavation step. The buckle in the curve takes place in the stage where the gaps close, starting in this point a higher inner pressure is simulated.

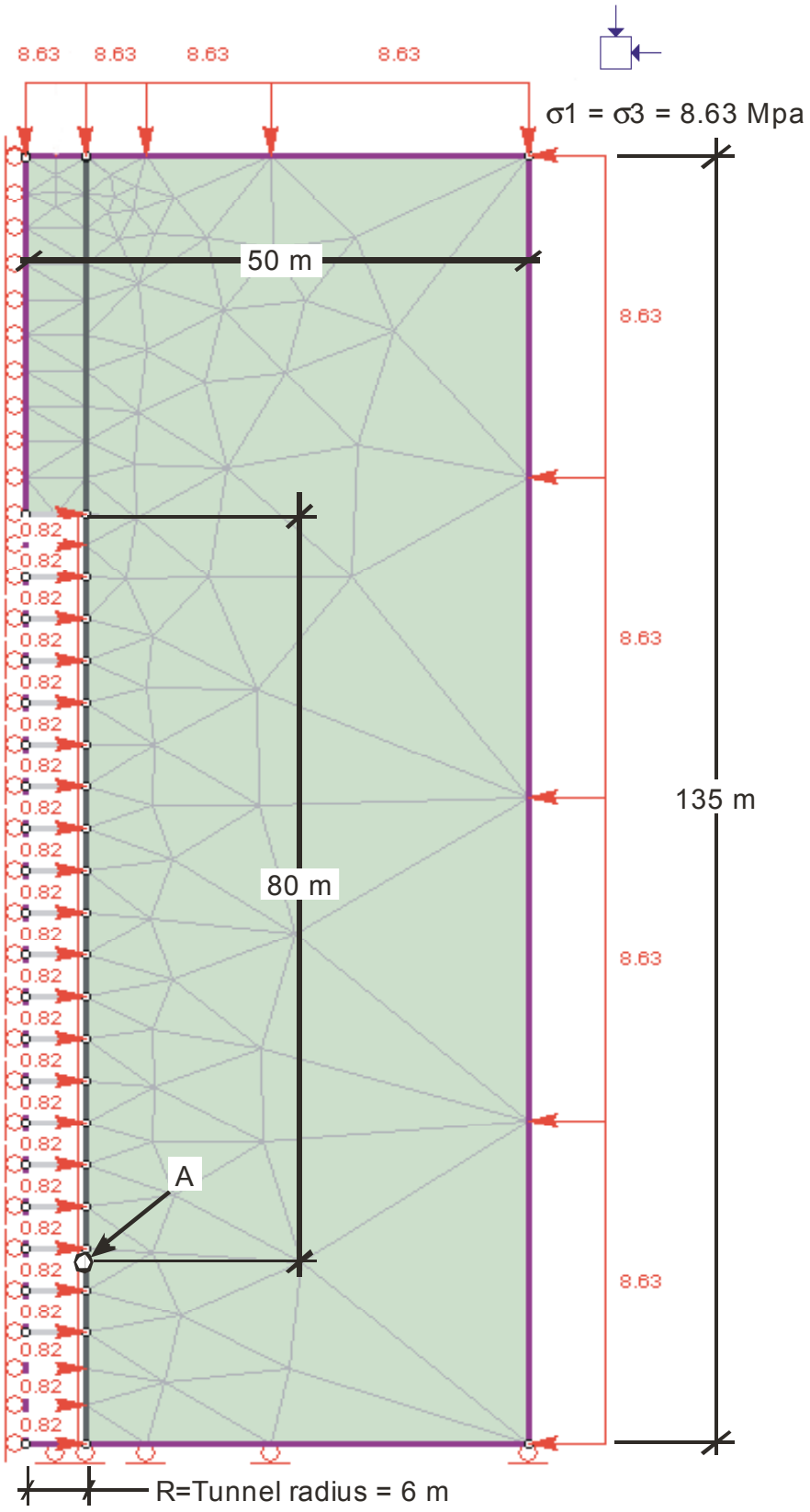

Fig. 20: Axisymmetric model K 0+685_ No open gaps

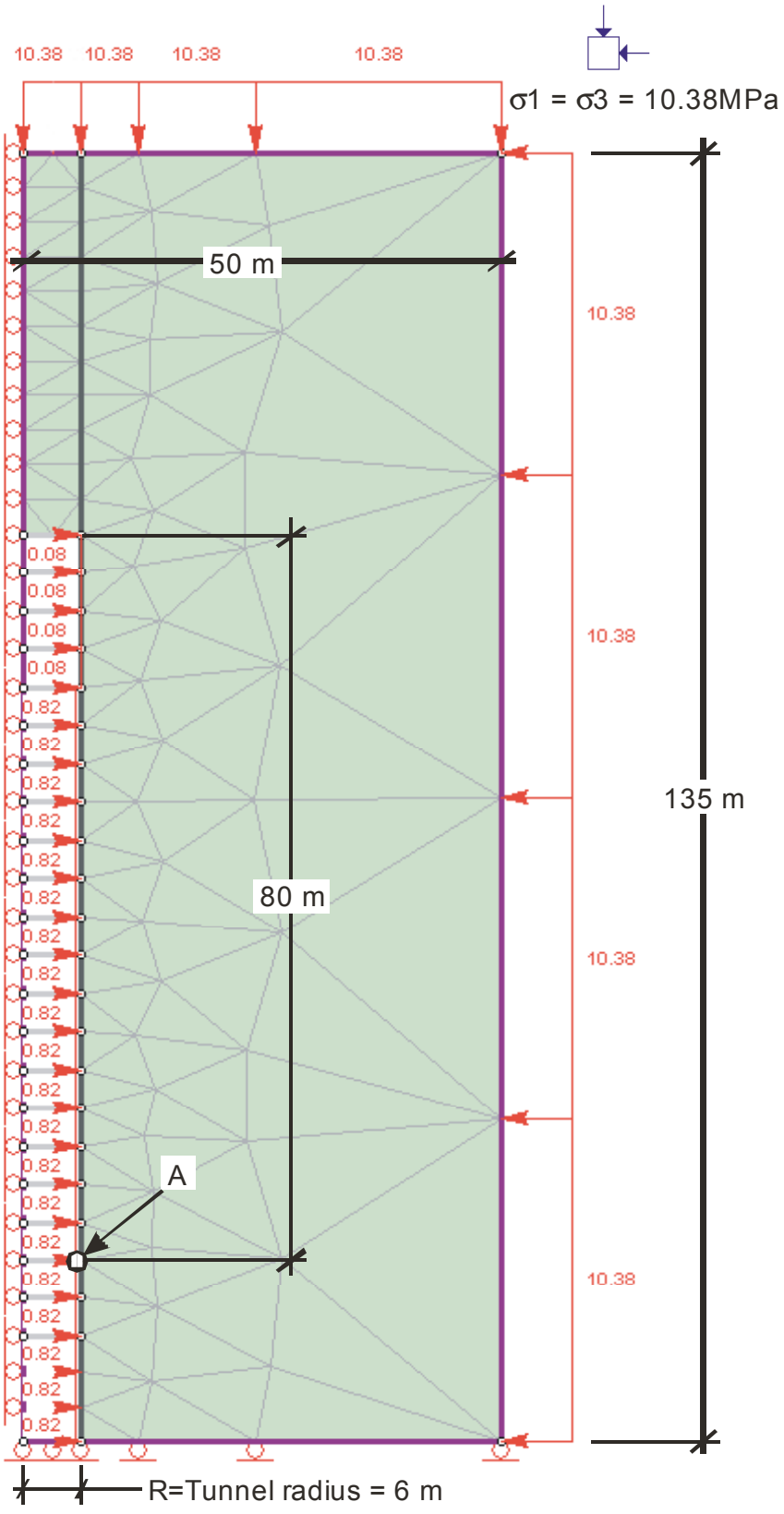

Fig. 21: Axisymmetric model K 2+748_ Open gaps

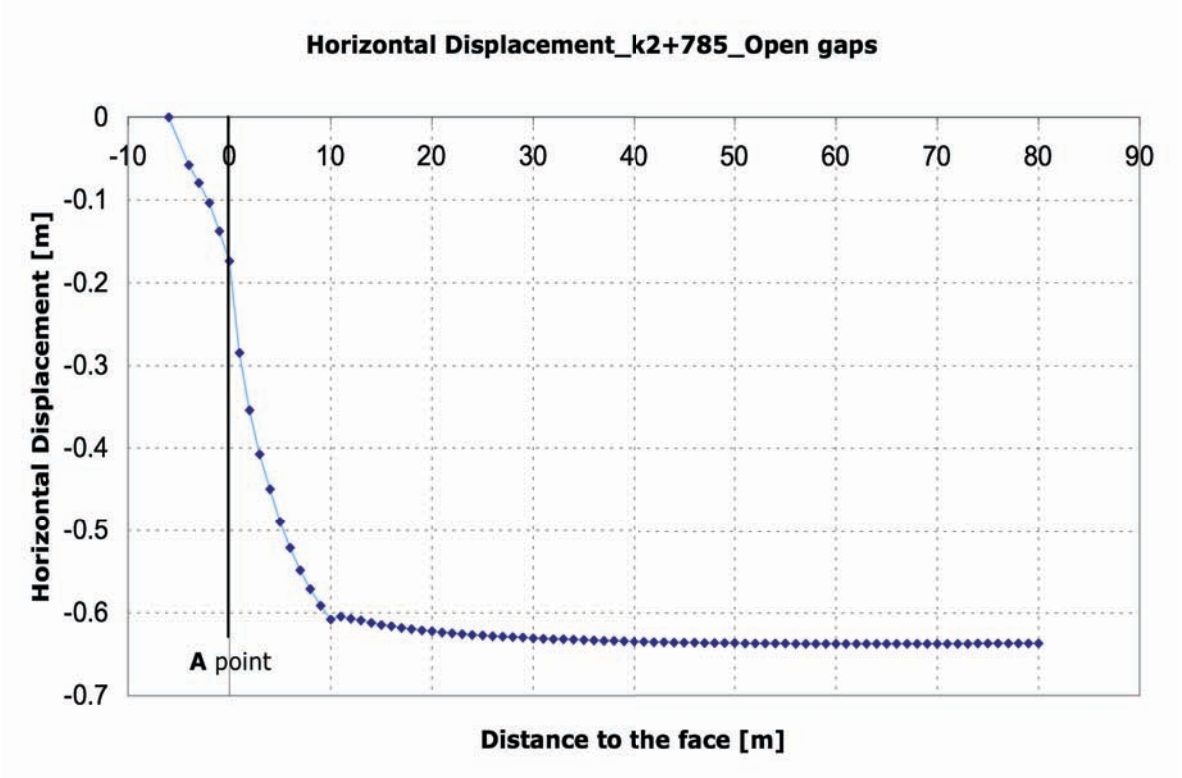

Fig. 22: Resulting displacements of the Axisymmetric model K 2+785_ Open gaps

The purpose of the simulation was to establish the displacement developed with the excavation advance for each set of parameters (E-c-φ) delivered by Matlab and then compare it to the one registered in situ (Geofit curves). An example of this process is shown in Fig. 23.

Even though the simulation would show a good “fitting” for some set of parameters, after several simulation it was concluded that, when the grouted bolts have big influence (large displacements are taking place) the model would not deliver the expected final displacement and therefore a wrong displacement path comes as a result.

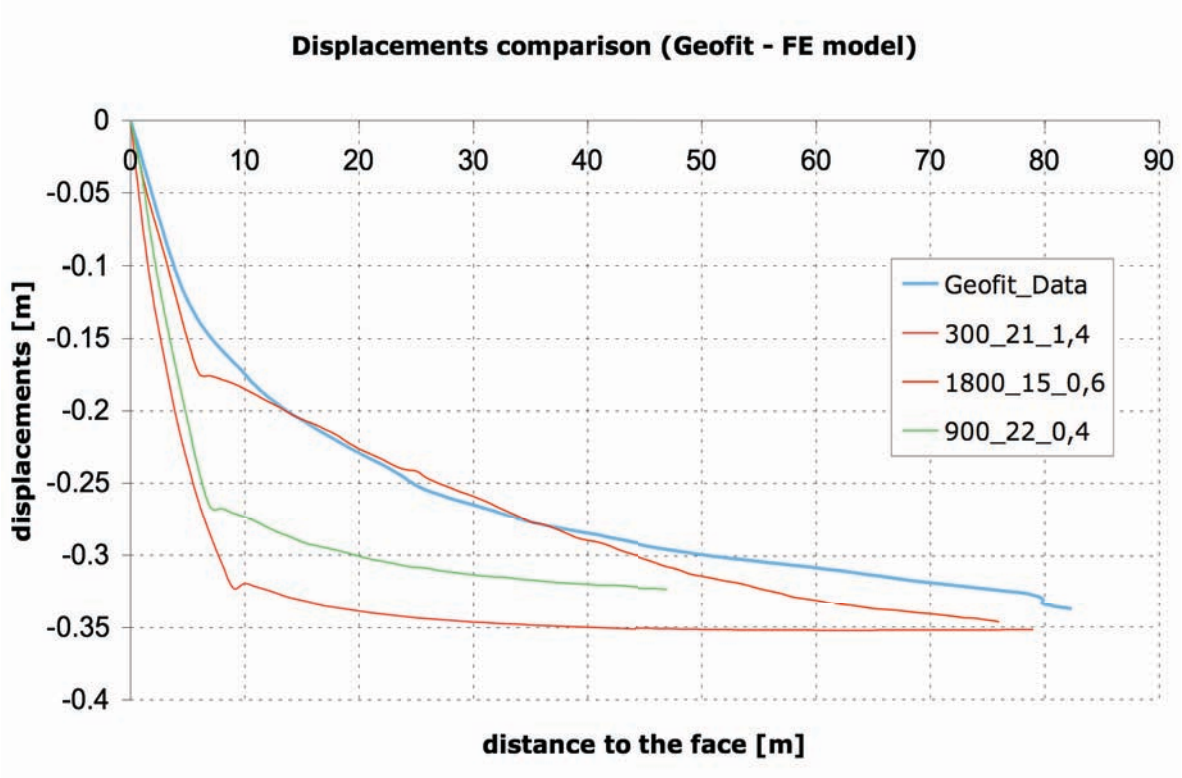

Fig. 23: Displacement development comparison_FE_K 2+785_ Open gaps

5.2.2. Formulation after Panet & Guenot [24]

The convergence analysis from Panet & Guenot [24] has the same conditions as the convergence-confinement method: circular cross section, homogeneous, isotropic and an elastic medium. The researchers studied the progressive closure behind the face as the face advances, basically a three-dimensional problem that through some simplification and uncertainties could be approached as an equivalent plane strain problem. Following expression (18) concludes their work, varying the closure of the tunnel as a function of the distance to the face and the plastic radius:

$$c(x) = c_{\infty}\left[1 - \left(\frac{1}{1 + \frac{x}{0.84 r_p}}\right)^2\right] \tag{18}$$

where:

x is the distance to the tunnel face [m];

C_{∞} is the maximal radial displacement [m];

r_p is the plastic radius [m].

Taking the formulation of Panet & Guenot [24] and the plastic radius delivered by the Matlab back analysis, as a starting point, one could see the set of parameters that fit better to the measured displacements. As seen in Fig. 24, 25 and 26, for the cross sections k0+685, k2+748 and k3+307 respectively, the measured displacements and the ones calculated by the formulation from Panet & Guenot [24] show good fitting. It is worth mentioning that the cross section with the lowest overburden (k1+651) had the worst fitting when compare to the other cross sections.

Once the plastic radii that fit best to the measured displacements were identified, the corresponding set of E-c-φ is known, through this process it was possible to minimize the range of the back calculated values. Table 6 summarizes these values.

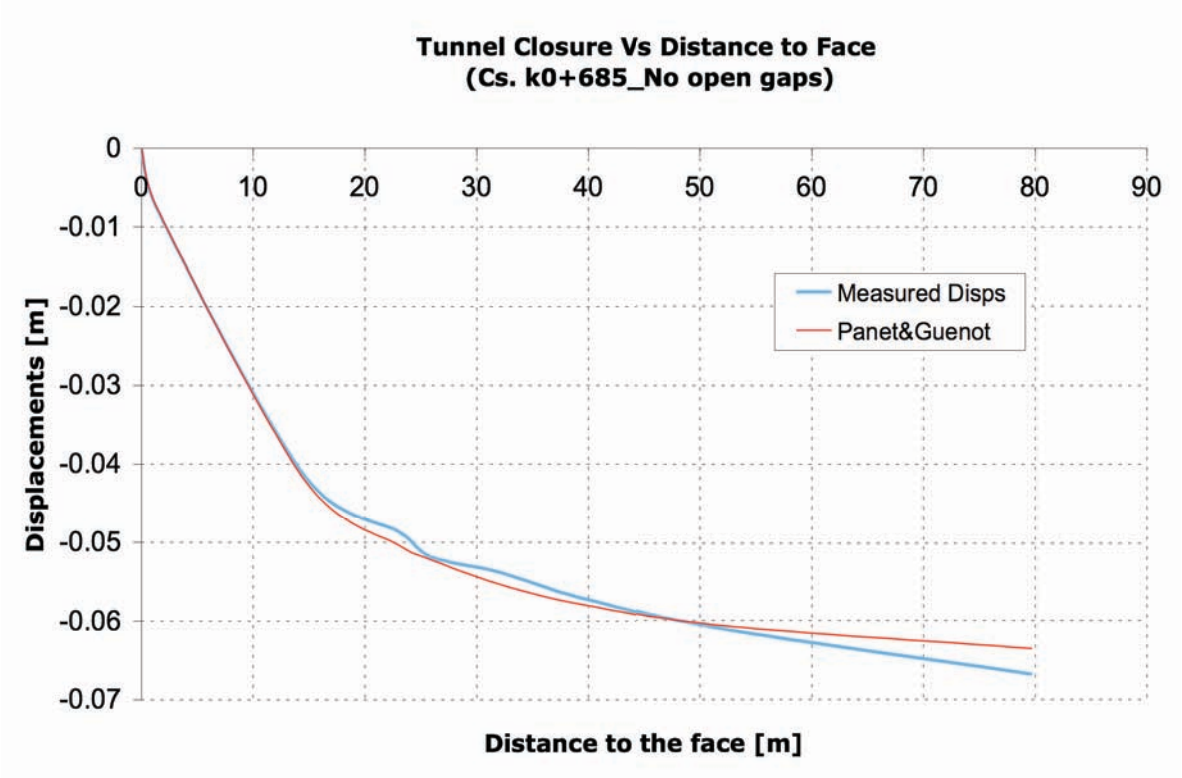

Fig. 24: **Displacement development comparison_Panet & Guenot [24] k 0+685_No open gaps**

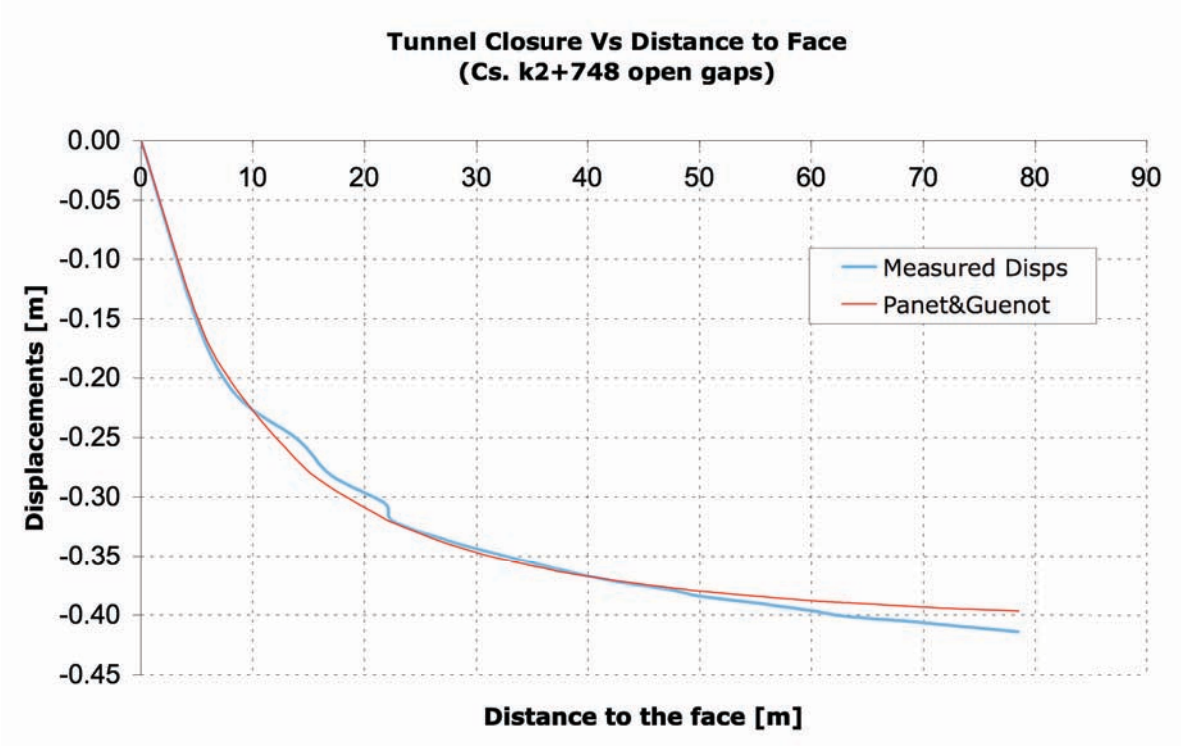

Fig. 25: **Displacement development comparison_Panet & Guenot [24] k 2+748_Open gaps**

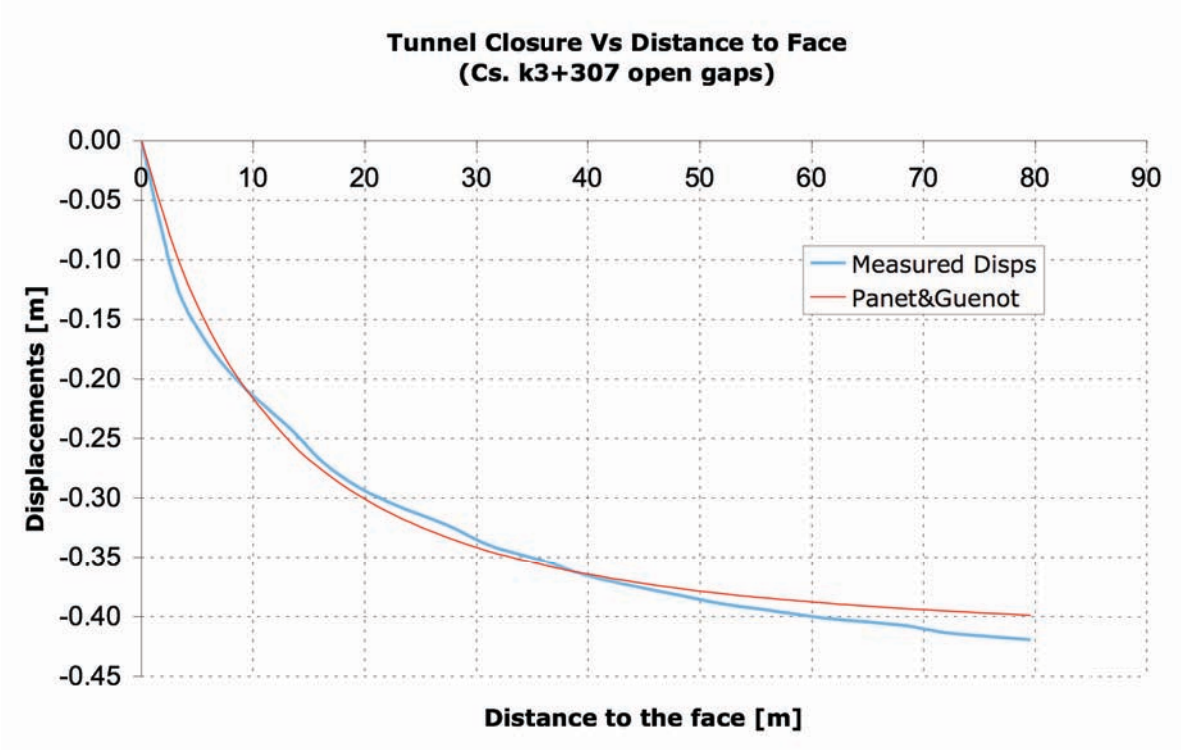

Fig. 26: **Displacement development comparison_Panet & Guenot [24] k 3+307_Open gaps**

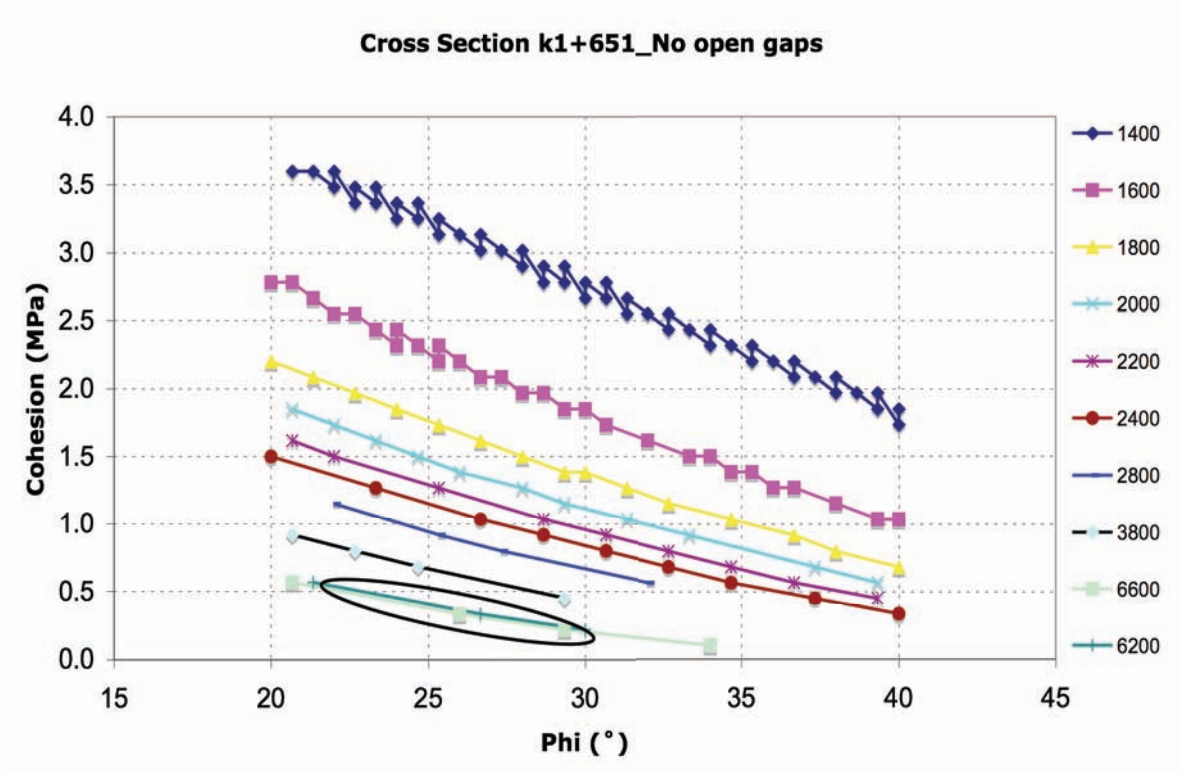

Fig. 27: **Back analyzed range values_K 1+651_No open gaps**

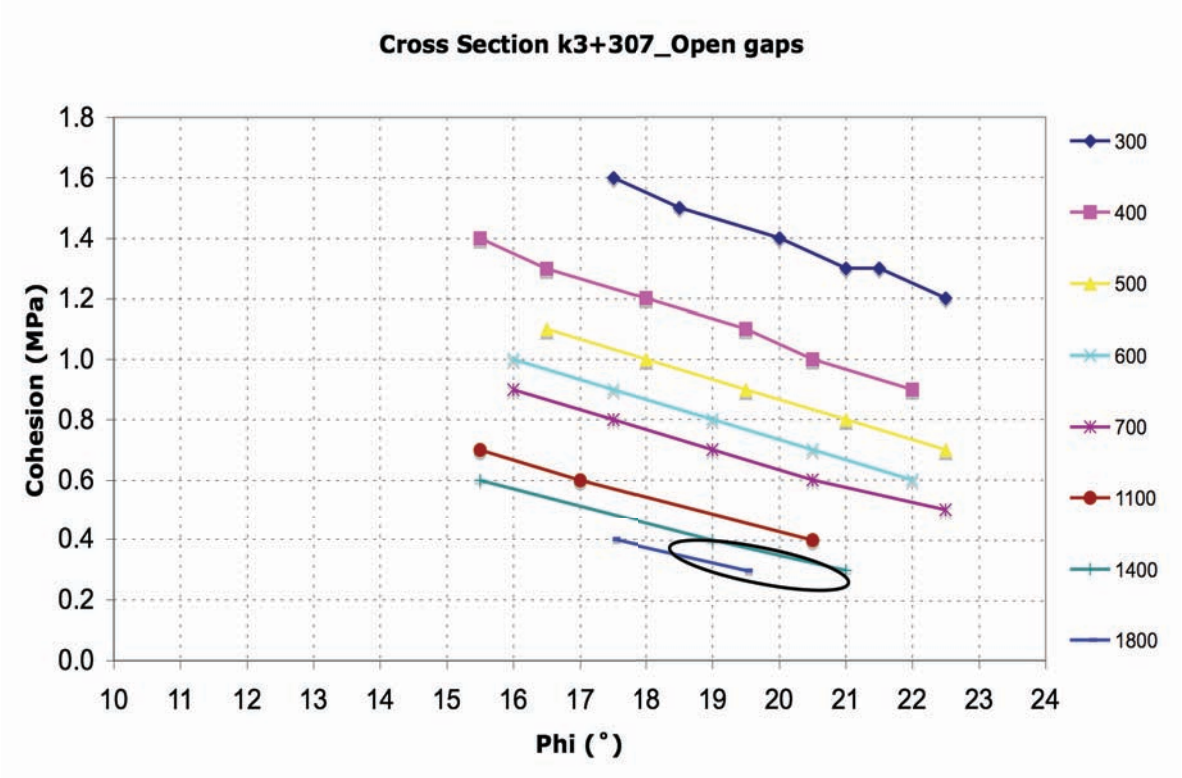

Fig. 28: Back analyzed range values_K 3+307_Open gaps

Fig. 27 and 28 are shown as an example for the range of values' selection in cross sections k1+651 and k3+307 respectively. It is worth mentioning that the values shown in Table 6 are to be considered as range therefore all E-c-φ values between those ranges fulfill the displacements (Matlab simulation) and Plastic Radius (Panet & Guenot [24] formulation) conditions.

	E (MPa)	**Phi** (˚)	**C** (MPa)	**PlasticRadius** (m)
k0+685	1200	19.0	0.3	25.52
	1300	18.5	0.3	26.89
	1300	20.5	0.2	26.56
k1+651	6200	21.3	0.6	16.05
	6600	20.7	0.6	16.77
	6600	26.0	0.3	16.43
	6600	29.3	0.2	16.28
k2+680	2900	20.0	0.3	27.62
	2900	22.5	0.2	27.22
k2+748	1100	19.5	0.3	24.27
	1100	21.5	0.2	24.02
	1200	19.0	0.3	25.52
	1200	21.0	0.2	25.23
k2+785	1700	19.5	0.3	25.07
	1800	19.0	0.3	26.39
k3+224	700	20.0	0.5	19.56
	800	19.0	0.5	21.26
	900	20.0	0.4	22.62
k3+242	1400	20.0	0.3	27.10
	1500	19.5	0.3	28.56
	1600	21.5	0.2	28.88
k3+307	1400	21.0	0.3	24.05
	1500	18.5	0.4	25.53
	1800	19.5	0.3	27.94
k3+558	2000	22.5	0.4	16.14
	2200	20.0	0.5	17.15

Table 6: Summarized Range values for the Inntal Tunnel.

5.3. Influence of Young's modulus

In order to find out the influence of the Young's modulus, the back analyzed parameters where studied towards E-c-φ combination behavior. To accomplish this purpose a linear regression was calculated for every single E in a given cross section. From this procedure the parameters *a* and *b* from the formulation of a linear function y = ax + b were calculated (Table 7) these parameters a and b describe the influence of different Young's moduli. Therefore the graphics in Fig. 29, 30 and 31 show the resulting *a* and *b* values and depict a quadratic function in order to describe this data. These graphics are not to be compared, as they are from different cross sections with different overburdens and support systems, that is why no trend can be detected analyzing the different a and b values.

Cross Section k1+651				Cross Section k2+748				Cross Section k3+307			
E	a	b	Correl	E	a	b	Correl	E	a	b	Correl
1400	-0.094	5.589	-0.994	300	-0.076	2.543	-0.999	300	-0.078	2.948	-0.995
1600	-0.090	4.552	-0.996	400	-0.073	2.233	-1.000	400	-0.076	2.565	-0.998
1800	-0.085	3.887	-0.998	700	-0.067	1.767	-1.000	500	-0.067	2.200	-1.000
2000	-0.068	3.194	-0.996	800	-0.067	1.700	-1.000	600	-0.067	2.067	-1.000
2200	-0.063	2.875	-0.997	1000	-0.067	1.600	-1.000	700	-0.062	1.889	-0.998
2400	-0.059	2.622	-0.996	1100	-0.055	1.375	-0.999	900	-0.067	1.833	-1.000
2600	-0.056	2.472	-0.995	1200	-0.055	1.348	-0.999	1000	-0.057	1.614	-1.000
2800	-0.058	2.401	-0.996	1300	-0.055	1.320	-0.999	1100	-0.059	1.618	-0.999
3000	-0.051	2.182	-0.996	1600	-0.050	1.175	-1.000	1200	-0.055	1.503	-0.999
3200	-0.050	2.065	-0.997					1300	-0.054	1.452	-0.998
3400	-0.049	2.028	-0.995					1400	-0.055	1.448	-0.999
3800	-0.054	2.017	-0.999					1500	-0.057	1.457	-1.000
4000	-0.054	1.982	-0.999					1800	-0.050	1.275	-1.000
4200	-0.052	1.905	-0.999								
4800	-0.035	1.388	-0.991								
5400	-0.035	1.342	-0.991								
5800	-0.035	1.318	-0.991								
6200	-0.041	1.430	-0.998								
6600	-0.035	1.271	-0.991								

Table 7: Linear regression data.

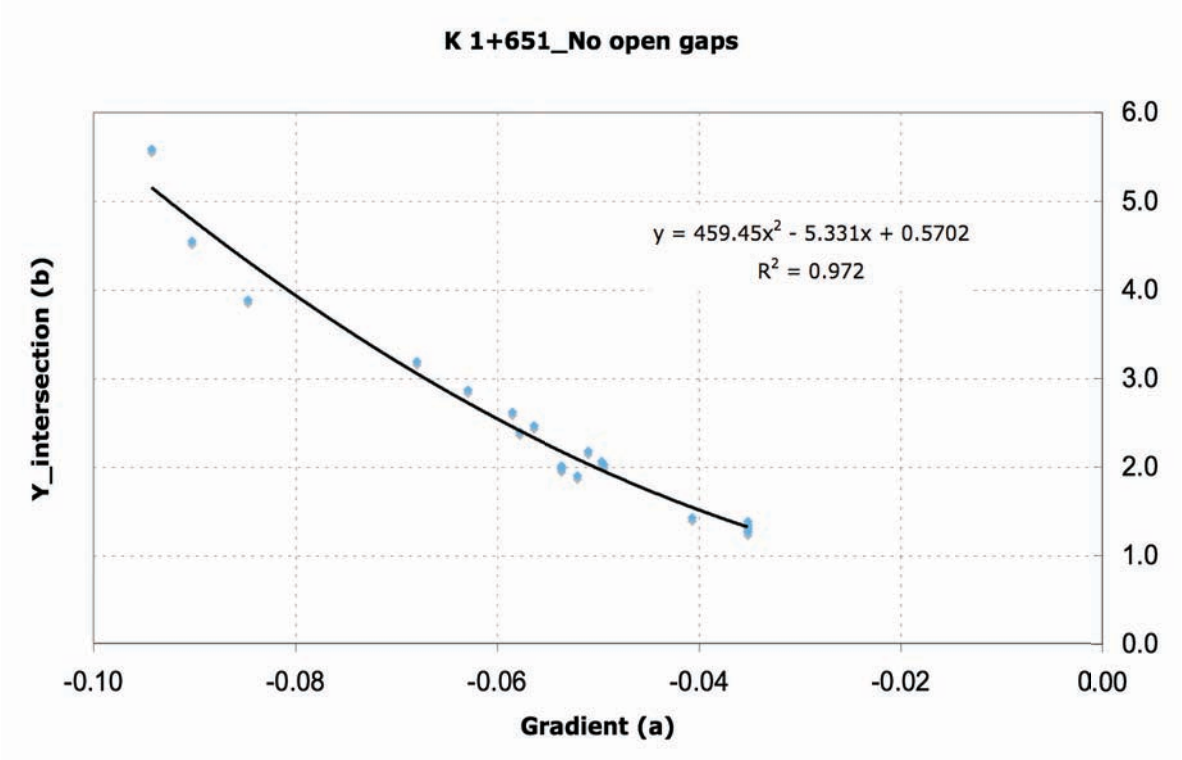

Fig. 29: **Quadratic regression for the back analized parameter_Cross section k 1+651_No open gaps**

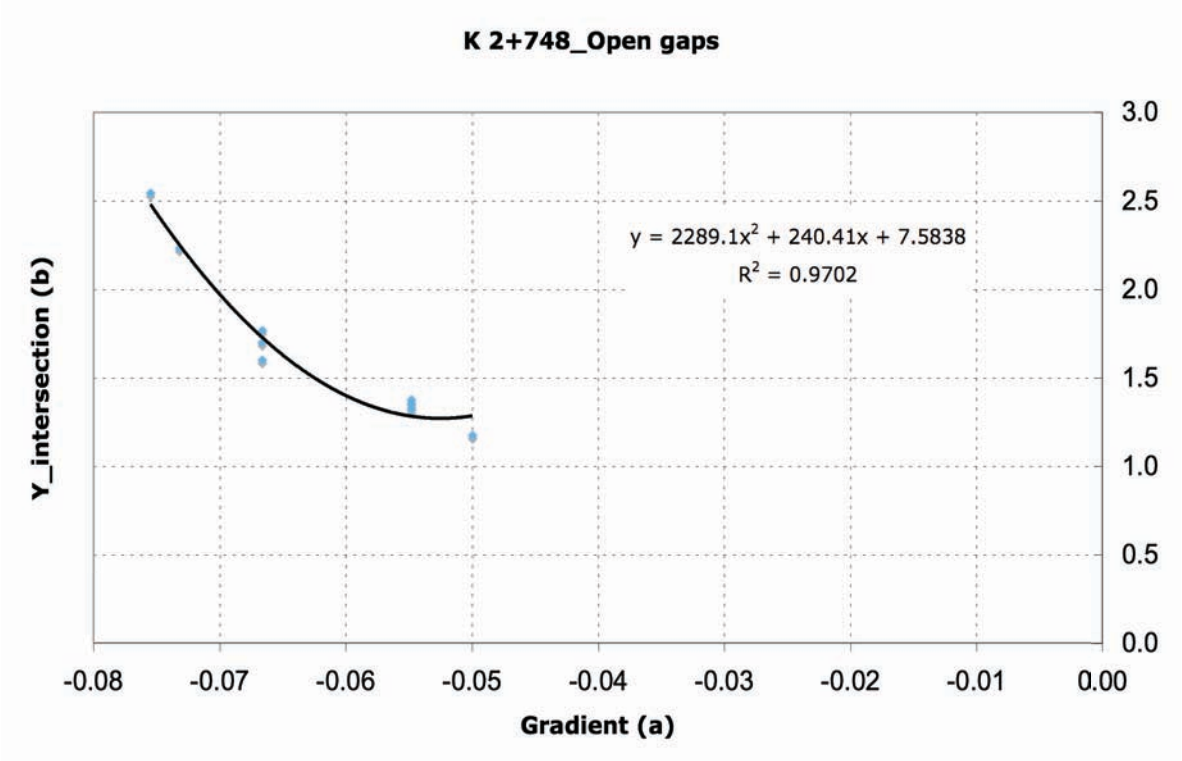

Fig. 30: **Quadratic regression for the back analized parameter_Cross section k 2+748_Open gaps**

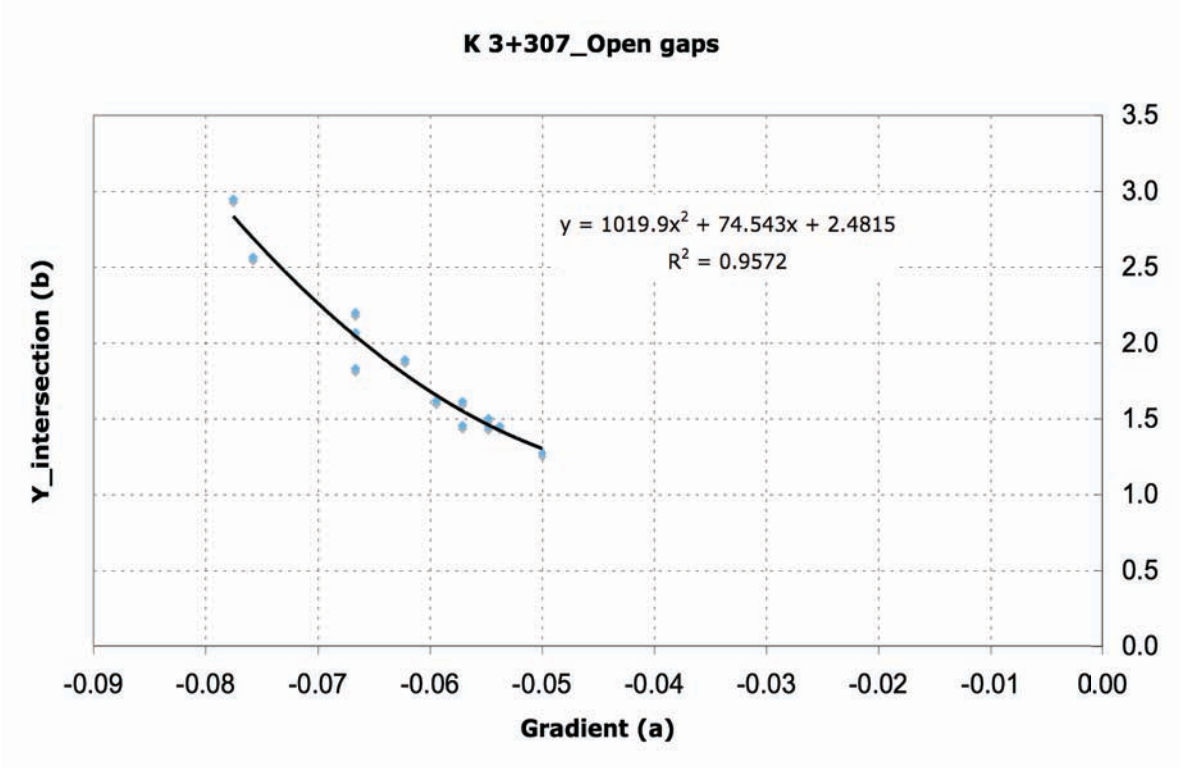

Fig. 31: Quadratic regression for the back analized parameter_Cross section k 3+307_No open gaps

Fig. 29, 30 and 31 show a trend that follows a quadratic equation in each cross section. It was observed that the Young's moduli are inversely proportional to the *a* values (gradient) and *b* values (intersection with the *y*-axis) in almost all cross sections where open gaps were used. In cross sections with no open gaps a trend can also be detected but only for low Young's moduli, the higher the Young's moduli are the more complicated to establish a trend. This can also be seen in Fig. 27 where high Young's moduli (bottom of the graphic) tend to have different gradients and intersect each other.

6. Discussion

6.1. Comparison to FE and Feder & Arwanitakis [1] calculations

The back calculated values were compared to the closed form solution after Feder & Arwanitakis [1] and to numerical FE simulations with Phase^2, both calculations proved the successful operation of the developed Matlab tool. Fig. 32 shows the cross section K0+685, which does not consider open gaps, implemented in phase^2. The displacements calculated from the formulation from Feder & Arwanitakis [1] as well as FE simulation, are in the same order of magnitude with the proposed model (see Table 8).

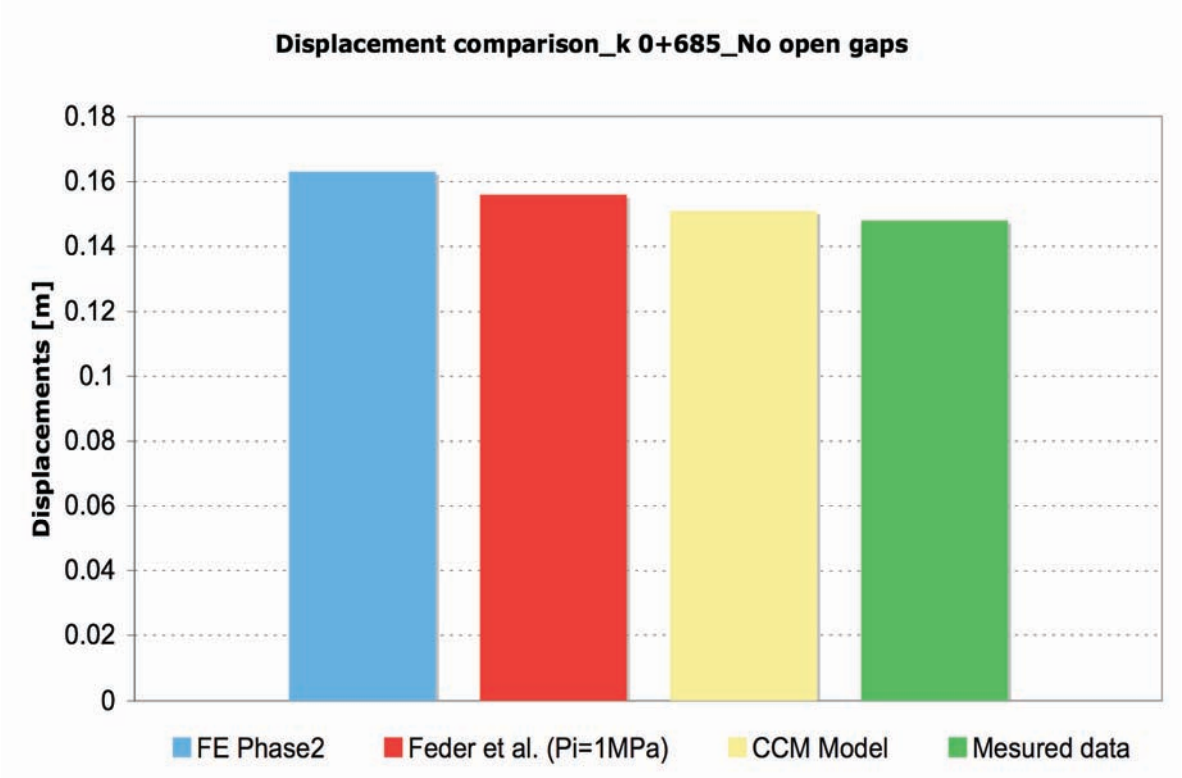

Fig. 32: Comparison of displacements of the used models

Cross section: k 0+685_No open gaps	
Model	**Displacement [m]**
FE Phase2	0.163
Feder et al. (Pi=1MPa)	0.156
CCM Model	0.151
Mesured data	0.148

Table 8: Comparison of displacements of the used models.

6.2. Comparison between grouted and non grouted bolts

Even though the use of non-grouted bolts and cables is not a common practice in tunneling nowadays, the Matlab code developed for this thesis allows the user to simulate a SCC considering this kind of support. Taking this into account the present study compares the usage of grouted and non-grouted bolts. For this purpose several analysis were made varying the amount, longitudinal spacing, length and diameter of the bolts, as well as the E, c and φ rock mass parameter. It has to be considered that the diameter of a non grouted bolt was always smaller compared to a grouted bolt. In the case of grouted bolts the external diameter of the grouting is also an input value for the model.

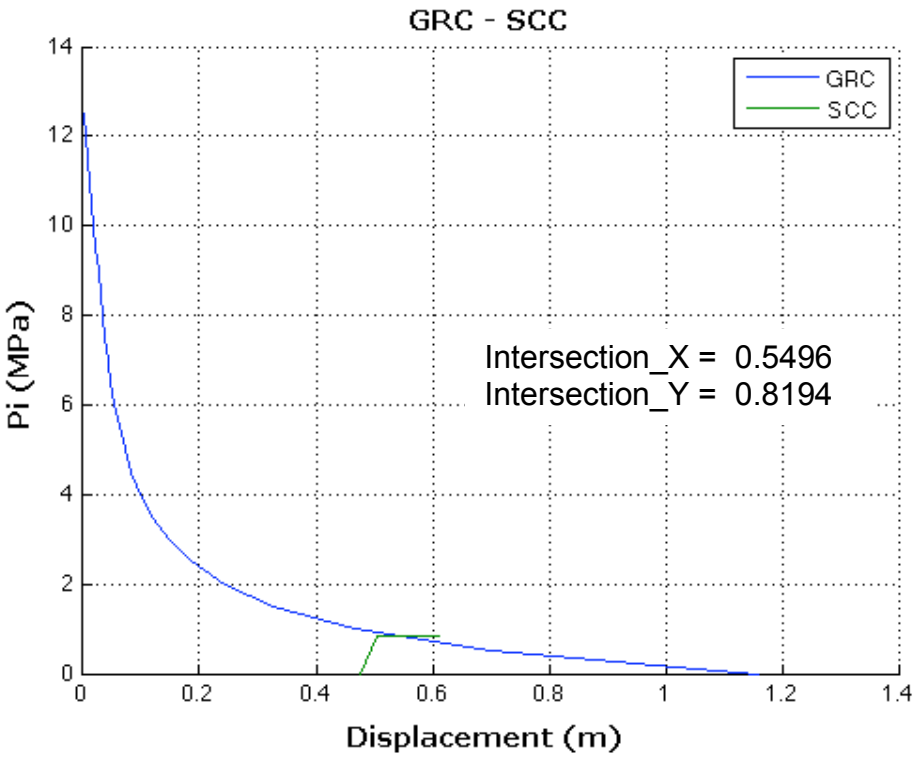

Fig. 33: **GRC and SCC for support with Grouted bolts**

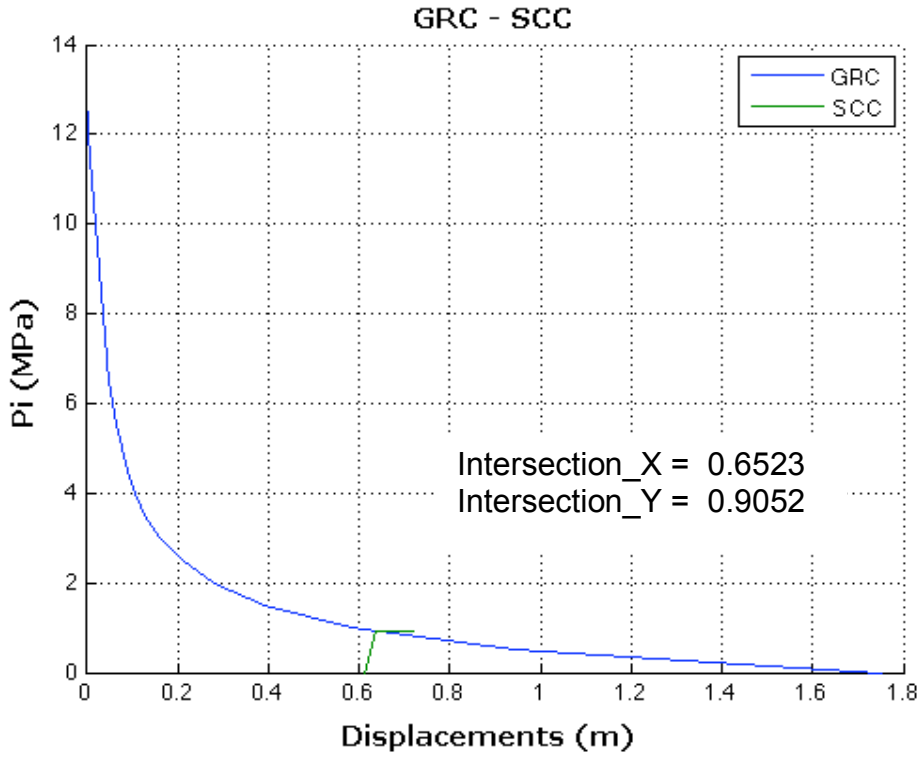

Fig. 34: **GRC and SCC for support with Non-Grouted bolts**

It was seen that when using the same number, length and diameter of bolts for a specific rock mass defined by E, c and φ the final displacement values are always lower in the case of the grouted bolts (see in Fig. 33 and 34).

For the specific case shown in Fig. 33 and 34 an overburden of 500m, E=1000MPa, c=0.5MPa, $\varphi=20^{\circ}$ and a support system consisting of 20cm shotcrete and a total of 25 bolts were selected (steal profiles are not considered in this section).

Comparing the two scenarios a ratio of ≈1.2 was calculated, that would hypothetically imply that ≈30 non-grouted bolts would reach the same final displacement as 25 grouted bolts. This ratio applies only for this specific case, since, for the grouted bolt case, the load is transferred and distributed throughout the length of the bolt and proportional to the rock mass displacements. But the same trend can be seen in all analyzed calculations.

Comparing different cases of grouted bolts and cases without any bolts the dependency of the grouted bolts on the rock mass displacements was also seen in this analysis. The perceptual difference in the final displacement (equilibrium point) increases inversely proportional to the rock quality and overburden, in other words the less competent the rock mass the better is the effect or contribution of the grouted bolts.

The presented model does not consider dilatancy for grouted bolt cases, nevertheless it is worth mentioning that dilatancy contributes to stability as mentioned in the previous chapter.

7. Conclusions

There are many reasons why back analysis models are used more frequently e.g. better and more reliable algorithms are available, the possibility of implementing them in simple personal computers in which one can produce large amounts of data, quick response to unexpected events and low cost among others.

The proposed model gives the possibility to assemble the convergence-confinement method for rock masses that satisfy Mohr Coulomb failure criteria in short time and with low computational requirements, almost all support systems in tunneling are available and results are presented in a simple and comfortable manner.

The specific study for the Inntal tunnel, as expected, gives a wide range of values that fulfill the final displacement condition, due to the mathematical formulation used in the model, however as in the back-analysis techniques presented by Shang et al. in [7] and Yang et al. in [8] the analyzed data has to be selected based on experience. In order to decrease the range two approaches were implemented, the approach based on the formulation after Panet & Guenot [24] fits best to support system design for the specific case. Through the formulation presented by Panet & Guenot [24] the presented model is able to deliver quality data regarding E, c and φ peak values based on observed displacements.

It was seen that proposed model do not show a good fitting for cross sections with low overburden and small displacements, further studies regarding this subject should be done, since only one cross section (k1+651) with these characteristics was analyzed in the present study.

One important consideration comes into mind when analyzing a further application of the presented model. As a common practice laboratory and in situ testing

focuses mainly on c, E and φ peak values making these values relatively easy and inexpensive to obtain. However, as explained by Alejano and Alonso in [22], dilatancy and strength parameters in residual conditions are most difficult to estimate from preliminary investigations. In this scenario the back analysis model could be used to calculate dilatancy or an equivalent parameter, which describes the strain behaviour of the rock mass in plastic conditions, having E, c and φ values as input parameters.

8. References

[1] Feder G., Arwanitakis M.: Zur Gebirgsmechanik ausbruchnaher Bereiche tiefliegender Hohlraumbauten; Austria; (1976)

[2] Hisatake M., Hieda Y.: Three dimensional back analysis method for the mechanical parameters of the new ground ahead of a tunnel face; Kinki University; Department of Civil and Environmental Engineering; Japan; (2007)

[3] Xia-Ting F., Hongbo Z., Shaojun L.: A new displacement back analysis to identify mechanical geo-material parameters based on hybrid intelligent mythology; The Chinese Academy of Science; Institute of Rock and Soil Mechanics; PR China; (2003)

[4] Fakhimi A., Salehi D., Mojtabai N.: Numerical back analysis for estimation of soil parameters in the Resalat Tunnel project; New Mexico Institute of Mining and Technology Mineral Engineering Department; USA; (2003)

[5] Oreste P.: Back analysis techniques for the improvement of the understanding of rock in underground construction; Politecnico di Torino, Department of Georesources and Land; Italy; (2004)

[6] Shunsuke S., Shimichi A., Kunifumi T., Masato S., Norikazu S.: Back analysis for tunnel engineering as a modern observational method; Hiroshima Institute of technology; Japan; (2003)

[7] Shang Y., Cai J., Hao W., Wu X., Li S.: Intelligent back analysis of displacements using precedent type analysis for tunneling; Nanyang Technological University, Singapore; (2002)

[8] Shang Y., Yang J., Hao W., Li S.: Intelligent back analysis of displacements monitored in tunneling; Chinese Academy of Sciences, Institute of Geology and Geophysics; PR China; (2006)

[9] Vardakos S., Gutierrez M., Barton N.: Back analysis of Shimizu Tunnel No. 3 by distinct element modeling; Virginia Polytechnic Institute and State University; Department of Civil and Environmental Engineering; USA; (2006)

[10] Amusin B., Shick V., Lama R.: Using Back Analysis to estimate geotechnical field parameters for the design of support systems for tunnels; Tunneling and Underground Space technology; Vol. 7; Great Britain.

[11] Oreste P.: Analysis of structural interaction in tunnels using the convergence confinement approach; Politecnico di Torino, Department of Georesources and Land; Italy; (2004)

[12] Zhang L., Yue Z., Yang Z., Qi J., Liu F.: A displacement-back analysis method for rock mass modulus and horizontal in situ stress in tunneling; The University of Hong Kong; Department of Civil Engineering; PR China; (2005)

[13] Petrovitsch H.: Inbetriebnahme der Umfahrung Innsbruck. Schienenverkehr aktuell; Austria; (1994)

[14] Kainrath S., Gschwandtner G., Galler R.: The convergence confinement method as an aid in the design of deep tunnels; Geomechanics and Tunneling, Vol 2, Germany; (2009)

[15] Hook E., Carranza-Torres C., Diederichs M.S., Corkum B.: Integration of geotechnical and structural design in tunneling; Geotechnical Engineering Conference; USA; (2008)

[16] Indraratna B., Kaiser P.: Design of grouted rock bolt based on the converge control method; Int. J. Rock Mech. Min. Sci. & Geomech, Vol. 27. No. 4. pp. 269-281; Great Britain; (1990)

[17] Oreste P.: Distinct analysis of fully grouted bolts around a circular tunnel considering a congruence of displacements between the bar and the rock; Politecnico di Torino, Department of land, Environment and Geotechnology Engineering ; Italy; (2004)

[18] Carranza-Torres C., Fairhurst C.: Application of the Convergence-Confinement Method of Tunnel Design to Rock masses that satisfy the Hoek-Brown failure criterion; Tunneling and Underground Space technology; vol 15. No. 2; (2000)

[19] Stille H., Holmberg M., Nord G.: Support of Weak Rock with Grouted Bolts and Shotcrete; Royal Institute of Technology, Department of Soil And Rock Machanics; Sweden; (1989)

[20] Radoncic. N., Schubert. W., Moritz B.: Ductile support design; Geomechanics and Tunneling, Vol 2, Germany; (2009)

[21] Hoek E., Carranza C., Diederichs M., Corkum B.: The 2008 Kersten lecture integration of geotechnical and structural design in tunneling; Annual Geotechnical Engineering Conference; USA; (2008)

[22] Alejano A., Alonso E.: Considerations of the dilatancy angle in rocks and rock masses; University of Vigo, Natural Resources & Environmental Engineering Department; Spain; (2005)

[23] Pöttler R.: Über dei Wirkungsweise einer geschlitzten Spritzbetonschale; Felsbau 15, No. 6, Germany; (1996)

[24] Panet M., Guenot A.: Analysis of convergence behind the face of a tunnel; Laboratorie Central des Ponts et Chaussees, Institut of Mining and Metallurgy; France; (1982)

[25] Guan Z., Jiang Y., Tanabasi Y.: Ground reaction analyses in conventional tunneling excavation; Nagasaki University; Department of Civil Engineering; Japan; (2007)

[26] Seller P.: Prediction of Displacements in Tunneling; Graz Institute of Technology; Department of Civil Engineering; Austria; (2000)

[27] Seeber G.: Druckstollen und Druckschaechte; Leopold Franzens Universitaet Innsbruck; Institut fuer Wasserbau; Austria; (1999)

[28] Martin D., Chanderl N.: The progressive fracture of Lac du Bonnet granite; International Rock. Mech. Min. Sci and Geomech.; Vol 31 No. 6; Great britain; (1994)

[29] Cai Y., Esaki T., Jiang Y.: An analytical model to predict axial load in a grouted rock bolt for soft rock tunneling; Nagasaki University, Department of Civil Engineering, Japan; (2004)

[30] Oreste P., Peila D.: Radial Passive Rockbolting in Tunneling Design with a New Convergece-Confinement method; Politecnico di Torino, Department of Georesources and Land; Italy; (1996)

[31] Hoek E., Brown E.: Practical estimates of rock mass strength. Int. J. Rock Mech. Sci. Geomech. Abstr; USA; (1997)